

Intermediate pyrolysis of wheat straw and softwood pellets

by

Bijay Dhakal

A thesis submitted in partial fulfillment of the requirements for the degree of

Master of Science

Department of Mechanical Engineering
University of Alberta

© Bijay Dhakal, 2021

Abstract

Rapid population growth and booming urbanization play an active role in world fuel demand. Today, primary fuel resources like coal and petroleum fulfill most of the energy supply and are the leading contributors to greenhouse gas (GHG) emissions. Biomass-based fuel technology can play a crucial role in reducing GHG emissions, because, as a renewable source, biomass can be converted into solid and liquid biofuels and these are nearly carbon neutral over its life cycle. Thermo-catalytic reforming (TCR[®]) is a thermo-chemical conversion process by which biomass can be converted into valorized products like bio-oil, biochar, and syngas and is based on intermediate pyrolysis. Conventionally, biomass is converted into bio-oil via various other thermochemical processes such as fast pyrolysis, gasification, hydrothermal processing and combustion; integrating intermediate pyrolysis and the post-reforming reaction are novel features of the TCR[®] process. A 2 kg/h lab scale unit (TCR-2) was used for the thermo-catalytic reforming for different feedstocks to convert organic material into valorized products like bio-oil, biochar, and syngas.

In the first part of this study, the thermo-catalytic reforming performance of wheat straw pellets was explored. The experiments were carried out in a reactor temperature range of 400 to 550 °C and a reformer temperature range of 500 to 700 °C. Bio-oil yield decreased with an increase in reactor or reformer temperature. The highest yield of bio-oil (8.43 wt.%) was obtained at 400 and 500 °C reactor and reformer temperatures. The lowest yield was obtained at 450 and 700 °C reactor and reformer temperatures, respectively. The bio-oil produced has a very low TAN (7.3 mg KOH/g) and low viscosity (3.9 mPas) at 550 and 700 °C reactor-reformer temperatures. At a high temperature, polyaromatic hydrocarbons (PAHs) and monoaromatic hydrocarbons (MAHs) increase, showing the better quality of the bio-oil at a higher temperature. The maximum higher

heating value (HHV) of bio-oil is obtained at 35 MJ/Kg, and oxygen content in the bio-oil is below 9%. The syngas produced has very high hydrogen content (36.32 vol.%) at reactor-reformer temperatures of 450 and 600 °C, and the biochar produced has a very low O/C and relatively high H/C ratio.

In the second part of the study, Canadian softwood pellets were subjected to TCR[®] experiments, and products were tested for qualitative and quantitative performance. Softwood feedstock was tested at a fixed reformer temperature of 700 °C and a fixed reactor temperature of 400 °C. The maximum bio-oil (7.994 wt.%) was found at a reactor temperature of 400 °C and reformer temperature of 500 °C. The bio-oil produced is of superior quality with very low TAN and viscosity (3.14 mg KOH/g and 11.9 mPas, respectively). The char showed excellent stability with a very low O/C ratio and relatively high H/C ratio. The highest hydrogen content was observed at a reactor temperature of 500 °C and reformer temperature of 700 °C. Finally, the HHV of the bio-oil produced was recorded in the range of 37.5 MJ/Kg. Low TAN and viscosity, and very low oxygenated compounds in the bio-oil as compared to fast pyrolysis oil showed better stability and minimum downstream post processing required for utilization. High hydrogen content in the syngas and high HHV of biochar showed potential applications in the power generation.

Preface

This thesis is an original work by Bijay Dhakal under the supervision of Professor Amit Kumar.

Chapter 2 of this thesis, titled “Thermo-catalytic reforming of Canadian agricultural residue and advance characterization of final products,” by Bijay Dhakal, Vinoj Kurian, Rajender Gupta, Jason Olfert and Amit Kumar, will be submitted to a peer-reviewed journal.

Chapter 3 of this thesis, titled “Parametric optimization of thermo-catalytic reforming of softwood pellets to produce biofuels,” by Bijay Dhakal, Vinoj Kurian, Manjot Gill, Rajender Gupta, Andreas Hornung, and Amit Kumar, will be submitted to a peer-reviewed journal.

I was responsible for all the experimental work, data collection, qualitative and quantitative data analysis, and manuscript composition. Vinoj Kurian reviewed the experiments, assessed the results, and provided feedback on the research structure. He also corrected journal papers along with Astrid Blodgett, the editor of the research group. Professor Amit Kumar was the supervisory author and played a key role in overall supervision, conceptualization, planning, analysis and validation of results and manuscript edits.

For Buwa and Aama

Acknowledgments

First of all, my sincere gratitude to my graduate research supervisor, Professor Amit Kumar, for his constant guidance throughout this MSc journey. His encouragement, timely feedback, and profound knowledge played a prime role in my growth as a student and a researcher. I would also like to convey my thanks to Astrid Blodgett for her editorial suggestions and for editing my journal papers and thesis.

I want to thank the Ministry of Jobs, Economy and Innovation (earlier called as Ministry of Economic Development, Trade, and Tourism), Alberta Innovates, WestJet, the Fraunhofer Institute for Environmental, Safety and Energy Technology – UMSICHT (FGh-UMSICHT), the Future Energy Systems (a Canada First Research Excellence Fund) and the University of Alberta for financial support for this research.

I would also like to express my sincere thanks to Dr. Vinoj Kurian for his immense assistance in the lab whenever needed and his teaching and invaluable suggestions during the research. I thank Dr. Kurian for his insightful reviews of my research work and for providing suggestions to improve my research. I want to express my thanks to Manjot Gill for training me on the operation of micro-GC, TAN, and the viscosity analyzer and providing all the external contacts needed to complete the analysis of the analytical part of my work. I would also like to thank Omex Mohan for his support during the grinding and pelletization process and for helping me brainstorm several issues.

Finally, I would like to thank the Sustainable Energy Research Group members for their camaraderie and knowledge-sharing, making my stay at the University of Alberta memorable. I would also like to thank my parents, brothers, sisters, friends back home, and Rashmi for their immense support during this process.

Table of Contents

Chapter 1: Introduction	1
1.1 Background	1
1.2 Research Objectives	6
1.3 Scope and Limitations	7
1.4 Thesis Outline	7
Chapter 2: Thermo-catalytic reforming of Canadian agricultural residue and advance characterization of final products.....	9
2.1 Introduction.....	9
2.2 Materials and methods	12
2.2.1 Feedstock preparation and pelletization.....	12
2.2 Experimental setup.....	14
2.3 Operating conditions	16
2.4 Analysis and measurements	16
2.4.1 Feedstock analysis	16
2.4.2 Bio-oil analysis	17
2.4.3 Syngas analysis	18
2.4.4 Biochar analysis	18
2.5 Results and discussion	18
2.5.1 Mass and energy balance	18
2.6 Effect of reformer temperature	20
2.6.1 Mass balance	21
2.6.2 Biochar characterization	23

2.6.3 Bio-oil characterization.....	24
2.6.4 Permanent gas composition and properties.....	28
2.7 Effect of reactor temperature	30
2.7.1 Mass balance.....	30
2.7.2 Biochar characterization	32
2.7.3 Bio-oil characterization.....	33
2.7.4 Permanent gas composition and properties.....	39
2.8 Conclusion	40
Chapter 3: Parametric optimization of thermo-catalytic reforming of softwood pellets to produce biofuels.....	42
3.1 Introduction.....	42
3.2 Material and methods.....	45
3.2.1 Feedstock characterization.....	45
3.2.2 Experimental setup.....	47
3.2.3 Product analysis and measurement	48
3.3 Results and discussion	49
3.3.1 Mass and energy balances.....	49
3.4 The effect of reformer temperature.....	52
3.4.1 Biochar characterization	53
3.4.2 Bio-oil characterization.....	54
3.4.3 Permanent gas composition and properties.....	58
3.5 The effect of reactor temperature.....	60
3.5.1 Biochar characterization	61

3.5.2 Bio-oil characterization.....	62
3.5.3 Permanent gas composition and properties.....	67
3.6 Conclusion	68
Chapter 4: Summary, conclusions, and recommendations for future work.....	70
4.1 Summary	70
4.2 Conclusions.....	74
4.3 Future work.....	76
References.....	77

List of Tables

Table 2.1 Operating conditions.....	16
Table 2.2. Mass balance.....	19
Table 2.3. Energy balance.....	19
Table 2.4. Post-reforming reactions.....	22
Table 2.5. Properties of biochar at a fixed reactor and variable reformer temperatures.....	23
Table 2.6. Ultimate analysis, HHV, TAN and viscosity of bio-oil produced at different reforming temperatures.....	25
Table 2.7. Summary of GC-MS analysis results at fixed reactor and different reforming temperatures.....	25
Table 2.8. Detailed GC-MS results with bio-oil produced at a variable reforming temperatures for agricultural residues	26
Table 2.9. Comprehensive permanent gas analysis at the fixed reactor and variable reformer temperatures.....	29
Table 2.10. Biochar characterization for a fixed reforming temperature of 600 °C.....	33
Table 2.11. Ultimate analysis, TAN, viscosity, and HHV of bio-oil at fixed reformer temperatures of 600 and 700 °C.....	34
Table 2.12. GC-MS analysis of bio-oil produced at a fixed reformer temperature of 600 °C.....	36
Table 2.13. Comprehensive gas analysis at a fixed reformer temperature of 600 °C.....	39
Table 3.1: Ultimate and proximate analysis of softwood pellets.....	46
Table 3.2. Operating conditions.....	48
Table 3.3. Mass balance of the TCR products from processing of softwood pellets	50
Table 3.4. Energy balance of the TCR products from processing of softwood pellets	51
Table 3.5. Post-reforming reactions (from Neumann et al. [43])	52

Table 3.6. CHNS analysis of softwood pellet-based biochar for a fixed reactor temperature and different reformer temperatures	53
Table 3.7. Softwood pellet-based bio-oil properties at a fixed reactor temperature of 400 °C	55
Table 3.8. GC-MS analysis of softwood pellet-based bio-oil at a fixed reactor temperature and different reformer temperatures	55
Table 3.9. Total compound GC-MS analysis of softwood pellet-based bio-oil at a fixed reactor temperature and different reforming temperatures	56
Table 3.10. Micro GC gas composition with a fixed reactor temperature and different reformer temperatures	58
Table 3.11. CHNS analysis of softwood pellet-based biochar at a fixed reforming temperature and different reactor temperatures	62
Table 3.12. Proximate analysis results of softwood pellet-based bio-oil prepared at a fixed reforming temperature and different reactor temperatures	63
Table 3.13 Complete set of compounds detected by the GC-MS at a fixed reformer temperature and different reactor temperatures in processing of softwood pellet in a TCR unit	63
Table 3.14. Permanent gas detected by the Micro GC at a fixed reformer temperature and different reactor temperatures in processing of softwood pellets in a TCR unit	67

List of Figures

Figure 2.1 Hammer mill.....	13
Figure 2.2. Pelletizer and screen assembly	14
Figure 2.3. Schematic of TCR process: feed hopper (1), feeding screw (2), auger reactor (3), fixed bed reformer (4), condensers (5), bio-oil container (6), gas wash bottle (7), filters (8), gas analyzer (9)	15
Figure 2.4. Average energy conversion and losses for the biomass conversion.....	20
Figure 2.5. Product distribution at fixed reactor temperature of 400 °C and variable reformer temperatures	21
Figure 2.6. Major gas composition at a fixed reactor temperature	30
Figure 2.7. Mass balance at a fixed reforming temperature of 600 °C	31
Figure 2.8. Mass balance at a fixed reforming temperature of 700 °C	32
Figure 2.9. GC-MS analysis of bio-oil produced at a fixed reformer temperature of 600 °C	35
Figure 2.10. GC-MS analysis of bio-oil produced at a fixed reformer temperature of 700 °C	38
Figure 3.1. Softwood pellets	46
Figure 3.3. Mass balance of TCR products from processing of softwood pellet at different reformer temperatures	52
Figure 3.4. The main gas yields in processing of softwood pellets at a fixed reactor temperature and different reformer temperatures through a TCR unit	60
Figure 3.5. Mass balance at different reactor temperatures for processing of softwood pellets in a TCR unit.....	61
Figure 3.6. Set of compounds from the GC-MS analysis of softwood pellet-based bio-oil at a fixed reforming temperature and different reactor temperatures	66

Figure 3.7. The main permanent gas compositions for a fixed reformer temperature (700 °C) and different reactor temperatures in processing of softwood pellets in a TCR unit	68
Figure 4.1 TCR product yields from softwood and wheat straw pellets at a fixed reactor temperature of 400 °C	71
Figure 4.2 TCR product yields from softwood and wheat straw pellets at a fixed reformer temperature of 700 °C	71
Figure 4.3 TCR energy conversion data for softwood and wheat straw pellets at 500 °C (reactor) and 600 °C (reformer)	72
Figure 4.4 Viscosity, TAN, and HHV for wheat straw and softwood pellets at a fixed reactor temperature of 400 °C	73
Figure 4.5 Syngas composition comparison for wheat straw and softwood pellets at a fixed reforming temperature of 700 °C	74
Figure A- 1 Softwood and Wheat residue pellets biochar comparison at a fixed reactor temperature of 400°C	82
Figure A- 2 Softwood and Wheat residue pellets biochar comparison at fixed reformer temperature of 700°C	82
Figure A- 3 Comparison of GCMS analysis of wheat residue and softwood pellets at a fixed reactor temperature of 400 °C	83
Figure A- 4 Comparison of GCMS analysis of wheat residue and softwood pellets at a fixed reformer temperature of 700 °C	83
Figure A- 5 Syngas proportion comparison softwood and wheat residue pellets	84

List of Abbreviations

GHG	Greenhouse gas
NRCan	Natural Resources Canada
Mt	Million tons
TCR	Thermo-catalytic reforming
HHV	Higher heating value
LHV	Lower heating value
MSW	Municipal solid waste
IPP	Independent power provider
OECD	Organization for Economic Co-operation and Development
MW	Megawatt
GC	Gas chromatograph
TGA	Thermogravimetric analysis
GC-MS	Gas chromatography-mass spectrometry
DCM	Dichloromethane
TAN	Total acid number
NINT	National Institute for Nanotechnology
O/C	Oxygen/carbon
H/C	Hydrogen/carbon
PAHs	Polyaromatic hydrocarbons
MAHs	Monoaromatic hydrocarbons
FAMEs	Fatty acid methyl esters

Chapter 1: Introduction

1.1 Background

Fossil fuel consumption is increasing every year; Canada's greenhouse gas (GHG) emissions in 2019 were 730 million tons (Mt) CO₂ equivalent, 21.4% more than the total GHG emissions in 1990 [1]. This increase is primarily from transportation, oil and gas extraction, and building consumption. Canada has committed to reduce its GHG emissions to 30% of 2005 levels by the year 2030, or 219 Mt CO₂ equivalent. However, by 2019 Canada had reduced GHG emissions by only 9 Mt CO₂ from 2005 levels. Between 2005 and 2019, Alberta's GHG emissions increased by 40 Mt, or 17%. However, Ontario's GHG emissions decreased by 21% [1]. In 2018, 80,733 PJ of renewable energy was produced worldwide. Canada produces 3% (2,049 PJ) of this energy and ranks 7th in global renewable energy production. 67.5% of Canada's renewable energy is from hydropower, 23.3% from solid biomass (wood/waste), and 5.2% from wind power [2]. From 2000 to 2018, energy production from Canadian biomass was between 504 and 610 petajoules, and the primary source of biomass energy was solid and liquid wood waste [2].

Firewood and charcoal have long been in use. Recent advances in research have led to the production of transportation fuels from forest residues and fast-growing crop feedstocks. Forest residues include sawmill residues (off-cuts, sawdust, chips, bark), timber harvest leftovers such as treetops, branches, bark, thinning, etc., and sometimes waste from wood processing industries (furniture, construction, joinery)[3]. In 2017, an estimated 392 million dry tons of woody biomass was available to generate renewable energy. It is projected that by 2022 almost 12.4 million dry tons of forest residue will be used for energy purposes [4]. By 2050, biomass will provide about 50 to 450 exajoules of energy [5].

Lignocellulosic feedstock is the most abundant source of biomass in Canada. Lignocellulosic Biomass from agriculture and forestry operations is used to produce bioproducts and sustainable renewable energy. Around 27 million tons (Mt) of agricultural and forest residue biomass are used by over 200 Canadian firms [6]. Canada has an estimated 64-561 million dry tons of agricultural and forest residue potential per year [7] . Around 9% of the world's forests, i.e., 347 million hectares of forest, is in Canada; this represents almost 35% of Canada's land area. Canadian forests are mainly made up of the coniferous trees (68%), followed by mixed wood at 16% and broadleaf trees at 11% [7]. Most Canada's forests (76.6%) is owned by the provincial government, followed by territorial and private forests at 12.9% and 6.2%, respectively. As of 2016, almost 4.5% of the forest area was affected by insects, and only 766,659 hectares (<0.5%) was harvested [7] and these are also a potential source of lignocellulosic biomass. Almost 60% of Alberta's land is forested. Every year almost 23.5 million m³ of round wood is harvested in the province; this harvest generates 1.04 million bone dry tons of forest residue (10% of the total harvest). Almost 95% of roadside residue is burned to prevent wildfires each year [8]. In Canada in 2016, only 3.1% of the total renewable electricity was generated from forest biomass; this is 2% of the country's total electricity generation [7].

Agricultural waste generally refers to the remains of wheat, rice, maize or corn, barley, sorghum, millet, cotton, coffee, groundnut, jute, legumes, cacao, olives, tea, fruit, and palm oil after cultivation. Crop residues are agricultural wastes either left to rot or burned in the field after grain harvesting. These residues are seen as a renewable, and abundantly available valuable economic resource. A small portion of these residues are used as animal feed, soil nutrient, and the energy source for bioethanol conversion. The six main crops in the world are barley, rice, maize, sugar cane, soybean, and wheat. In 227 countries, these crops can provide 3.7×10^9 dry residue per year.

North and South America contribute significantly (500 million tons per year), and Eastern and Southern Asia produce over 200 million tons of agricultural residue per year [5].

Canada's annual agricultural residue potential is 25-48 million tons. After food and livestock feed use, wheat straw makes up a major portion of the total residue harvested in Canada [9]. 82% of Canada's cropland is in the Prairies, and 92% of the country's wheat is produced there [9]. From 2001 to 2010, the highest average agricultural residue available annually for biofuel production was from Saskatchewan (17.38 million dry Mg yr⁻¹), followed by Alberta at 11.58 million dry Mg yr⁻¹. British Columbia, P.E.I (Prince Edward Island), New Brunswick, and Nova Scotia play a small role in biofuel production [10]. Despite this great potential in Canada, ethanol production dominates (20 of 22 ethanol plants) first-generation (grain-based) technology [9].

Lignocellulosic biomass is the focus of increased research because it is a promising natural and renewable resource and is essential to modern industrial society's regular operation. Although it is natural and renewable, much of the lignocellulosic biomass is disposed of without the energy content being extracted. This feedstock can be converted to high-value products like bio-fuels, value-added chemicals, and cheap energy sources for fermentation and enzyme production [11]. Lignocellulosic feedstocks mainly consists of cellulose, hemicellulose, and lignin, as well as some extractives and inorganic ash. A typical plant cell is 30-50% cellulose, 15-35% hemicellulose, and 10-20% lignin by mass. Cellulose (C₆H₁₀O₅)_n is an unbranched homopolysaccharide at the molecular level consisting of 10,000-15,000 D-glucose. The D-glucose in cellulose is linked by β (1→4) covalent bonds, and another homopolysaccharide-starch is linked with α covalent bonds [12]. Numerous hydroxyl groups form hydrogen bonds in the same or vicinal chains interlinked by hydrogen bonds and Van der Waals forces, giving it high tensile strength. Cellulose has a different orientation throughout the structure and forms amorphous and crystalline regions [13].

In contrast, hemicellulose, a heteropolysaccharide consisting of C-5 and C-6 sugar branches, forms crystalline structures reinforced by hydrogen coding. The last constituent of lignocellulosic biomass is lignin; it is the second-most abundant polymer yet has little value for bioenergy production and acts as a mechanical support for biomass [12].

There are many ways of converting biomass into energy and usable chemicals including combustion, pyrolysis, gasification, and high-pressure liquefaction [14]. Pyrolysis converts biomass into solid charcoal, liquid (bio-oil), and syngas in the absence of oxygen by the thermal decomposition process. During this process, cellulose, hemicellulose, and lignin decompose over a broad temperature range through three significant stages: pre-pyrolysis, the main pyrolysis process, and solid char devolatilization [15].

Generally, based on the inert nitrogen environment, pyrolysis is divided into slow, intermediate, and fast pyrolysis. Final products like biochar, bio-oil, and syngas distribution during pyrolysis depend on primary factors such as reaction temperature, heating rate, and residence time [16]. Slow pyrolysis occurs at a low temperature of 350-550 °C, a slow heating rate of 0.01-80 °C/ min, and a high residence time of several minutes to hours or even days [17]. The primary aim of this process is to produce char. Torrefaction and carbonization are the two popular processes associated with slow pyrolysis. Torrefaction generally occurs at low temperature of 200-300 °C and carbonization occurs at a higher and broad temperature range [18].

Fast pyrolysis occurs at a high temperature of 1000 °C and a very high heating rate of 1000-10,000 °C/s. It has a very low residence time (<3 s). If bio-oil is the product of interest, peak temperature should be maintained below 650 °C [18]. It generally yields liquid bio-oil (60-75 wt. %), solid biochar (15-25 wt. %), and non-condensable gases (10-20 wt. %); these values are greatly affected

by the type of feedstock used [19]. Fast pyrolysis includes feedstock drying to <10% water content to ensure a rapid reaction and to reduce the final water content in the bio-oil, pyrolysis, rapid separation of solids, and rapid quenching for the collection of bio-oil. Though wood is the most popular feed for fast pyrolysis for its consistency and availability, over 100 kinds of feedstocks have been tested in laboratories including agricultural waste, energy crops, forest waste, sewage sludge, and leather waste.

Intermediate pyrolysis is carried out at a temperature of 350-550 °C, moderate heating rate of 200-300 °C/min, solid residence time of several minutes up to 10 minutes, and vapor residence time of 2-4 seconds. A high cooling rate for the vapor is needed to reduce the thermal energy post decomposition [20]. Intermediate pyrolysis has a typical product distribution of 50% liquid, 25% char, and 25% gas. The liquid produced from the fast pyrolysis of non-woody biomass shows much lower tar content and is compatible for direct application in boilers and engines. Bio-oil suitability can be further increased by the catalytic steam reforming of pyrolysis vapor to produce a considerable amount of hydrogen in syngas and further lower bio-oil viscosity. Similarly, the char produced is suitable for soil conditioning, carbon sequestration, and co-firing in the thermal plant [21].

Though fast pyrolysis is the most cost-efficient route to convert biomass into liquid fuel, it is less desirable because of the diverse nature of the components in the final product. Because of shortcomings like a short lifetime, aging, high viscosity, and the corrosive nature of the bio-oil produced, it needs to be upgraded to make it compatible to use directly in existing infrastructure [22]. To overcome these shortcomings, Fraunhofer UMSICHT introduced thermo-catalytic reforming technology (TCR[®]), the intermediate pyrolysis of feedstock in an auger reactor followed by post reforming [43]. TCR[®] yields solid biochar, hydrogen-rich syngas, and bio-oil with

excellent physical and chemical qualities [23]. The low oxygen content and the high energy density of TCR[®] bio-oil make it superior to other pyrolytic oils. Moreover, it is easier to transport and store TCR[®] bio-oil because of its high energy density [5]. Although TCR[®] is suitable for feedstock with a moisture content up to 70 wt. %, for the economy of the process, it is limited by the feedstock's higher heating value (HHV) and moisture content. Any feedstock with an HHV of 8 MJ/kg and a moisture content of less than 20 wt. % can be processed in this unit [23]. The following feedstocks have been tested in a lab-scale 2 kg/h TCR[®] plant: woody biomass [6], sugarcane bagasse [5], municipal solid waste (MSW) [5], sewage sludge [24], pulp rejects [24], agricultural residue (wheat husk) [25], spent coffee grounds [26], co-form rejects [5], digestate [23], and market waste [26].

In this research, agricultural and forest residues available in Alberta were tested in the TCR-2 (2 kg/h thermo-catalytic reformer) unit. These have not been tested earlier in a TCR[®] unit.

1.2 Research Objectives

With growing fossil fuel use, greenhouse gases are increasing significantly. The primary motive of this research is to find an alternative way of using biomass through experimental data. This research primarily uses lignocellulosic biomass to produce high-quality bio-oil, biochar, and hydrogen-rich syngas. The overall objective is to test the suitability of TCR[®] process in colder climates for biomass feedstocks available in Alberta. The following are the specific objectives of this research.

1. To study the effect of reactor and reforming temperatures on product yields (of bio-oil, biochar, and syngas) during the thermo-catalytic reforming of softwood pellets and wheat straw pellets in a laboratory-scale TCR-2 reactor.

2. To determine the optimal operating conditions to produce high-quality bio-oil, biochar, and syngas by performing qualitative and quantitative analyses of TCR[®] products.

1.3 Scope and Limitations

1. This study was performed on Canadian softwood pellets only and can be extended for hardwood pellets, a mixture of hardwood and softwood pellets, and wood chips. This study may help optimize the operating conditions for several forest residues and their derivatives.
2. In this study, only one agricultural residue (wheat straw pellets) was tested. This study could be extended for other types of agricultural residues such as canola straw, corn stover, and barley straw. A comparative study of different Canadian agricultural residues can also be done.
3. All the experiments in this work were performed at a fixed moisture content. A comparative study of feedstocks with different moisture contents can be performed and the effect of moisture content on the quality and quantity final products can be explored.

1.4 Thesis Outline

This thesis has four chapters; a summary of each is given briefly below. The format of the thesis is paper-based. Hence, each chapter has been written as an independent paper. Some of the introductory information in each of the chapters might be repeated.

The **first chapter**, the current chapter, comprises the introduction, research objectives, scope and limitations, and thesis outline.

The **second chapter** describes the comprehensive study of the thermo-catalytic reforming of wheat straw pellets and the advanced characterization of final products. The effects of reactor and reformer temperatures were studied, and the results are discussed. A comprehensive analysis of

bio-oil, biochar, and syngas was done, and following a quantitative and qualitative analysis of the results, the optimum temperature conditions for wheat straw pellets are suggested.

The **third chapter** describes the thermo-catalytic reforming of Canadian boreal forest residue-based softwood pellets. In this chapter, the effect of reactor and reformer temperatures on product yields was investigated, and a detailed characterization study of the TCR[®] products is reported. Based on the qualitative and quantitative analysis of the products, a suggestion is made on operating conditions.

The **final chapter** of this thesis gives the conclusions and recommendations for future work.

Chapter 2: Thermo-catalytic reforming of Canadian agricultural residue and characterization of final products

2.1 Introduction

Biomass is the organic material from plants and animals and contains energy directly or indirectly received from the sun. Until the mid-1800s, biomass was the primary source of energy consumption in the U.S. Developing countries still use biomass as a heat source. Biomass-based transportation fuels and electricity reduces greenhouse gas emissions over life cycle compared to fossil fuels [3]. Lignocellulosic biomass comprises of three main biopolymers: cellulose, hemicellulose, and lignin. Lignocellulosic biomass such as agricultural residues and forest residues can be used for production of energy and fuels [27]. Billions of tons of agricultural residues are generated worldwide each year, and majority of these are left in the field to rot or are burned [28]. Forest residues which are generated during the logging operation are burnt to prevent the forest fires. Both of these residues could be converted to fuels and electricity. In addition, the demand for paper has been decreasing and several of pulp and papers mills have closed. This also provides an opportunity for utilization of the whole tree biomass for production of energy and fuels.

Following the 2015 Paris Agreement, Canada promised to cut its greenhouse gas (GHG) emissions to 30% below 2005 levels by 2030[29]. Canada produced almost 730 Mt CO₂ equivalent in 2005, and if the country wants to fulfill its promise, it needs to reduce this to 511 Mt CO₂ equivalent by 2030. According to an Environment and Climate Change Canada estimate, oil and gas, electricity generation, heavy industry, and buildings will cut 104, 47, 46, and 44 Mt CO₂, respectively, by 2030. If these estimates are accurate, Canada is expected to generate only 503 Mt CO₂ equivalent by the end of that year[30]. To reach this goal, alternative and carbon-neutral sources of energy and fuels need to be explored and used.

In 2020-2021, Canada generated almost 16% of its energy from renewable sources [31]. The key players in renewable energy generation in Canada are hydropower and solid biomass (wood/waste); they comprise almost 91% of the total renewable energy generation. Majority of biomass-based power generation takes place in the pulp and paper mills. Other renewables like wind, solar, and thermal are becoming popular. In 2018, 36 operational co-generation units for pulp and paper industries and 41 other independent power providers (IPP) used biomass for their operation. In 2018, pulp and paper used 3427 MW for electricity generation and 1348 MW for heat generation, whereas IPP used 794 MW and 400 MW for electricity and heat, respectively [31]. In Canada, biomass contributes only 23% of the total renewable energy after hydro at 67.5%, yet in Organization for Economic Co-operation and Development (OECD) countries, it contributes almost 35% [31].

Lignocellulosic biomass is the primary biomass source in Canada. Forest and agricultural residues, which belong to the lignocellulosic group, can collectively contribute almost 27 million metric tons in Canada [6]. The prairie provinces (Alberta, Saskatchewan, and Manitoba), which comprise almost 82% of the total cropland in Canada, account for almost 15 million tons of agricultural residue each year. In addition, Canada has 347 million hectares of forests, which can contribute to the production of renewable feedstock [32].

Biomass can be converted to fuels through biochemical and thermochemical processes. Thermochemical conversion has an advantage over biochemical conversion because it converts biomass in a short time at high temperatures [33]. The key thermochemical processes for dry waste/biological residues are combustion, gasification, and pyrolysis. Combustion requires excess oxygen, and heat from the process can be used for electricity generation by producing steam [34]. Gasification of biomass takes place in limited supply of oxygen. In this process, carbon-based

feedstock is broken down into its basic constituents, which ultimately provides easy access to remove pollutants. At a high temperature and pressure, biomass reacts with oxygen to produce clean synthetic gas, which is efficient for electricity production [35]. Pyrolysis is thermochemical decomposition in the absence of oxygen, wherein lignocellulosic biomass is converted into a carbon-rich solid and volatile matter [36]. The volatile matter is condensed to produce bio-oil, a viscous dark liquid similar to fuel oil grade 2.

Depending on the heating rate and feedstock residence time, pyrolysis can be fast, intermediate, or slow [37]. Traditional pyrolysis (slow or fast) produces bio-oil which has problems like low thermal stability, a tendency to polymerize, high acidity, poor lubrication properties, ignition delay, high viscosity, and high water content. Specific adaptations need to be made to a burner to use bio-oil for energy production [38]. To tackle these problems, Pyroformer[®] was developed. Pyroformer[®], the first intermediate pyrolysis reactor, has an auger screw reactor comprised of two co-axially rotating screws. During pyrolysis, the outer and inner screws rotate together, some of the char is recycled with the fresh feed in the reactor. When the char is recycled, the oil produced is de-oxygenated with a low molecular weight, low water content, and low tar composition, with considerably improved qualities compared to traditional pyrolysis [39]. Intermediate pyrolysis continuously improved and evolved into the thermo-catalytic reforming (TCR)[®] process. TCR[®] combines intermediate pyrolysis with the post-catalytic treatment (reforming) process [39]. TCR[®] has two steps: first, intermediate pyrolysis in the horizontal reactor, where biomass is heated in the complete absence of oxygen at a mild heating rate and intermediate solid residence time. The second step is the reforming stage, where catalytic reforming occurs at elevated temperatures, leading to catalytic cracking of vapors. High-quality synthetic gas and organic vapor are condensed

into superior quality bio-oil with superior physical and chemical fuel properties compared to fast pyrolysis bio-oil [40-44].

The mass balance for the intermediate pyrolysis of wheat husk conducted by Santos et al. at 450 °C reactor and 600 °C reformer temperatures shows 5.8 wt. % bio-oil, 32.8 wt. % aqueous phase, 21.7 wt. % char, and 29.6 wt. % syngas. The bio-oil obtained has a very low total acid number (TAN) (29.9 mg KOH/g), low viscosity (145.2 cSt), and a very high higher heating value (HHV) (26 MJ/kg). The syngas produced has 19.4 vol. % hydrogen, 12.3 vol. % methane, 26.4 vol. % carbon monoxide, and 26.9 vol. % carbon dioxide and a very high HHV (20.6 MJ/m³) [39].

The main objective of the current study is to investigate the effect of reactor and reformer temperatures during the thermo-catalytic reforming of Canadian wheat straw pellets (agricultural residue) to produce bio-oil, biochar, and syngas. We also optimized operating conditions for the greatest yield and quality of TCR[®] products by advance characterization and analysis.

2.2 Materials and methods

2.2.1 Feedstock preparation and pelletization

Rectangular wheat straw bales (weighing roughly 20 kg) were collected from an agricultural biomass supplier in northern Alberta, Canada. The wheat straw residue was ground by hammer mill (model: SHM-5 manufactured by Kovo Novák, Czech Republic). A mesh size of 4 mm was used on the grinder to keep the ground product size less than 4 mm. The overall mass density of the loose feedstock was 85 kg/m³. The ground material was kept in a closed container for 24 hours to reduce non-uniformity in moisture distribution. Before pelletization, the die was preheated (and was later cleaned). The feedstock mixture for preheating the die was prepared by mixing 400 ml of water and 400 ml of canola oil with 4000 gm of ground feedstock. Half the feed was fed to the

pelletizer (model: BN4/7/10HP manufactured by Kovo Novák, Czech Republic) during the startup and the other half at the end of the process. The first batch of feed helps preheat the die used to produce pellets and the second batch of feed prevent clogging of the die for the next operation. After preheating, ground material was fed to the pelletizer to prepare enough pellets to perform the necessary number of experiments. When the pelletization process was complete, the pellets were stored in the open container for 24 hours to come to ambient conditions. The hammer mill and pelletizer used are shown in Figure 2.1 and Figure 2.2, respectively.



Figure 2.1 Hammer mill

A die of 6 mm inner diameter was used to produce pellets. The pellets have an average length of 19.02 mm with a standard deviation of 2.05 and a diameter of 6.12 mm with a standard deviation of 0.14. The bulk density of the pellets was found to be 672 kg/m³.



Figure 2.2. Pelletizer and screen assembly

2.2 Experimental setup

The thermo-catalytic reforming experiments were done in a 2 kg/h TCR[®] unit (TCR-2). TCR[®] technology was developed at Fraunhofer UMSICHT, Sulzbach-Rosenberg, Germany in 2013 [25]. The experimental setup used for this research is shown in Figure 2.3. The feed hopper, designed to hold 6 kg of pelletized feedstock, rests on top of the feeding screw, which prevents blockage and ensures the constant flow of feedstock to the reactor with the help of a pulsating motor attached to the end of the screw. The TCR[®] unit has three electric motors, eight primary heaters.

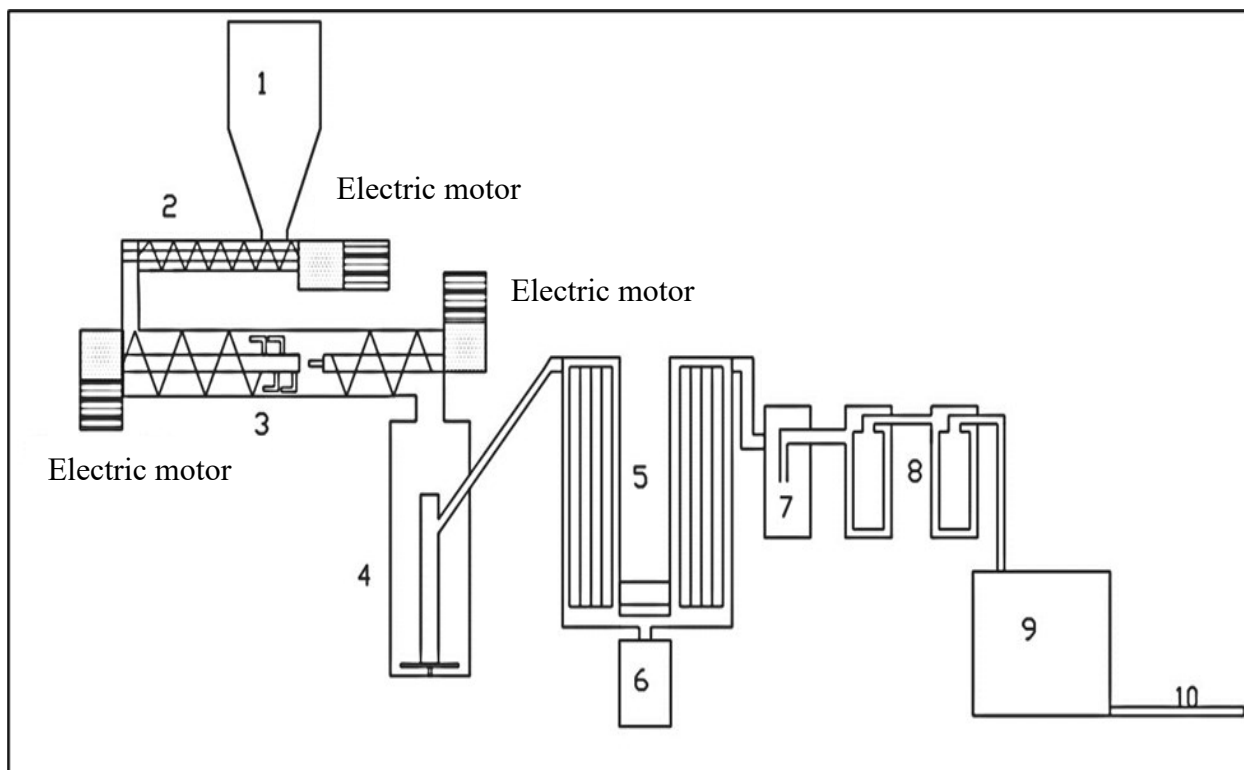


Figure 2.3. Schematic of TCR process: feed hopper (1), feeding screw (2), auger reactor (3), fixed bed reformer (4), condensers (5), bio-oil container (6), gas wash bottle (7), filters (8), gas analyzer (9)

The TCR-2's pyrolysis reactor is the horizontal unit equipped with two variable-speed motors on either end. It has two augers inside, and the auger on the incoming feed side has two subparts to mix a fraction of char with the incoming feed. When the speed of the motor mounted on each end is modified, the solid residence time in the reactor can be adjusted. The reactor has three major temperature zones; the first zone is maintained at 150-350 °C, the second zone is at 400-450 °C and the third zone is at 400-500 °C [37, 39, 42-48]. The vertical unit in the setup is the post-reformer, where pyrolysis vapor undergoes post-reforming reactions when it comes in contact with the produced char bed. The hot vapors then pass through two salient tube condensers, where the organic condensable fraction of the vapor is segregated from the permanent gas fraction. Bio-oil, along with the aqueous phase, is collected from the bottom of the condenser in the air-tight oil collecting vessel. Permanent gas goes through the wash bottle to remove aerosols and water-

soluble impurities. Permanent gas then passes through a series of filters (5 microns and 1 micron), then through a Y connection, which diverts some of the permanent gas for micro-GC analysis and the rest directly to the vent. A pressure transducer and thermocouple are provided at different locations to monitor the pressure and temperature profiles during experiments. The feedstock is heated inside the reactor and reformer with the help of electrical heaters encapsulated on the outer wall of the reactor and reformer tube.

2.3 Operating conditions

The operating conditions of the experiments were designed based on the temperatures of the reactor and the reformer. The guidelines were provided by the technology developer. A minimum temperature difference of 100 °C was maintained between the reactor and the reformer. The temperatures used in this study are shown in Table 2.1

Table 2.1 Operating conditions

Feedstock	Reactor temperature (°C)	Reformer temperature (°C)
Wheat straw pellets	400°C, 450°C, 500°C, 550°C	500°C, 600°C, 700°C

2.4 Analysis and measurements

2.4.1 Feedstock analysis

Both pellets and ground material were subjected to moisture analysis based on ASABE standard S358.2 (DEC93) [49]; at least 25 grams of feedstock was kept in an oven for 24 hours at 106 °C. Similarly, proximate analysis was done on LECO TGA 701 (make: LECO), following the ASTM D7582 standard (for moisture alone ASTM E1756-08) [50]; 1 gram of feed was kept at 107 °C until constant mass loss data was received. Finally, after we cross-verified the average of the data from the oven and the TGA, we calculated the overall moisture data. From the LECO TGA

proximate analysis, the fixed carbon, volatiles, and ash contents were also calculated. For fixed carbon and total volatiles, feed was heated in the absence of oxygen in a nitrogen atmosphere for 900 °C at a heating rate of 40 °C/ min and a holding time of 15 minutes. Finally, the remaining mass at 4 hours exposure at 575±25 °C in oxygen gave the total ash content of the feed.

The sample for ultimate analysis was prepared and analyzed using the Carlo Erba EA 1108 Elemental Analyzer. Carbon (C), hydrogen (H), and nitrogen (N) contents were calculated based on ASTM E777 [51] and ASTM E778 [52] standards, while sulfur (S) content in the feed was calculated based on the ASTM E775 standard [53]. Total oxygen (O) content was calculated based on the difference using the formula given in Equation 1.

$$O(\text{wt. \%}) = 100 - \Sigma \text{CHNS} (\text{wt. \%}) + \text{Ash}(\text{wt. \%}) \text{-----Equation 1}$$

2.4.2 Bio-oil analysis

The bio-oil sample was subjected to an ultimate analysis, GC-MS, pH, viscosity, and TAN. GC-MS was done using an Agilent 5975C mass spectrometer[54]. For the analysis, a 2 wt. % dichloromethane (DCM) solution was used, and compounds were identified using the NIST library for mass spectra [54]. The results were displayed in terms of relative abundance of peak area (i.e., % of peak area). Viscosity was measured through the ASTM D5018 method [55] using an Anton Paar rotational rheometer at 40 °C, and TAN was calculated as per the ASTM D664-04 standard [56] using Mettler Toledo T50 equipment. For TAN analysis, 0.25 gram of bio-oil solution was dissolved in the titration solution and treated with KOH (potassium hydroxide) to get the desired TAN value.

2.4.3 Syngas analysis

Continuous permanent gas analysis was done by an online micro gas chromatograph (GC model number CP-4900, make: Agilent) attached to the TCR[®] outlet. A 1-liter Tedlar bag was used to collect a sample every 30 minutes and store permanent gas for comprehensive analysis in a gas spectrometer on the day of the experiment. Both a micro- and a comprehensive GC analyzer were calibrated with the help of standard gas each day before the gas samples were analyzed. A micro-GC has a miniature GC with electronic carrier gas control, a micromachined injector, narrow bore analytic column, and micro thermal conductivity detector (μ TCD). It uses helium and argon as carrier gases and 2 out of 3 available columns for the experiment. The gas chromatograph (model number 7890 GC, make: Agilent) has two columns. It also uses argon and helium as carrier gases, and the micro-GC uses direct communication between the 7890 GC and 5977A series GC/MSD.

2.4.4 Biochar analysis

The biochar was subjected to moisture, proximate, and ultimate analysis as described in section 2.4.1.

2.5 Results and discussion

2.5.1 Mass and energy balance

Wheat straw residue pellets were fed in the 2 kg/hour lab scale TCR[®] unit. The yields of bio-oil, biochar, syngas, and the aqueous phase are listed in Table 2.2. The reactor's temperature ranged from 400 to 550 °C and the temperature in the reformer from 500 to 700 °C. The final product yields for bio-oil, biochar, and syngas were calculated by weight whereas the gas yield was calculated based on the difference. The bio-oil yield ranged from 1.78 to 8.43 wt. % . It decreased

with an increase in reactor or reformer temperature. The gas yield ranged from 31.81 wt. % to 55.0 wt. % and biochar yield from 26.62 to 30.15 wt. %.

Table 2.2. Mass balance

SN	Reactor temperature	Reformer temperature	Biochar %	Bio-oil %	Aq. phase %	Syngas % ^a
1	400	500	30.16	8.43	29.60	31.81
2	400	600	28.14	4.20	23.99	43.68
3	450	600	26.62	1.98	16.38	55.02
4	500	600	27.69	3.83	20.91	47.56
5	400	700	27.37	2.94	22.65	47.04
6	450	700	26.53	1.78	18.50	53.18
7	500	700	26.56	2.07	17.96	53.40
8	550	700	26.54	2.30	16.05	55.10

^a Calculated by the difference

Energy balance was determined by considering mass balance and the heating value of each product and is shown in Table 2.3. The TCR[®] process is endothermic, hence external heat is required to complete the reactions. Because of the lab-scale size of the reactor and the high heating demand, the electrical energy required for the setup is significant. Boundary conditions were set around the final products obtained from the setup only.

Table 2.3. Energy balance

S	Reactor temperature	Reformer temperature	% Bio-oil	% Biochar	% Syngas	% Conversion	% Losses
1	400	500	16.95	38.44	15.71	71.10	28.90
2	400	600	8.79	33.78	29.37	71.95	28.05
3	450	600	4.22	30.09	37.06	71.37	28.63
4	500	600	8.12	34.56	30.04	72.73	27.27
5	400	700	5.99	35.68	33.98	75.65	24.35
6	450	700	3.75	30.40	39.22	73.36	26.64
7	500	700	4.55	32.11	39.58	76.24	23.76
8	550	700	4.90	30.50	40.21	75.61	24.39

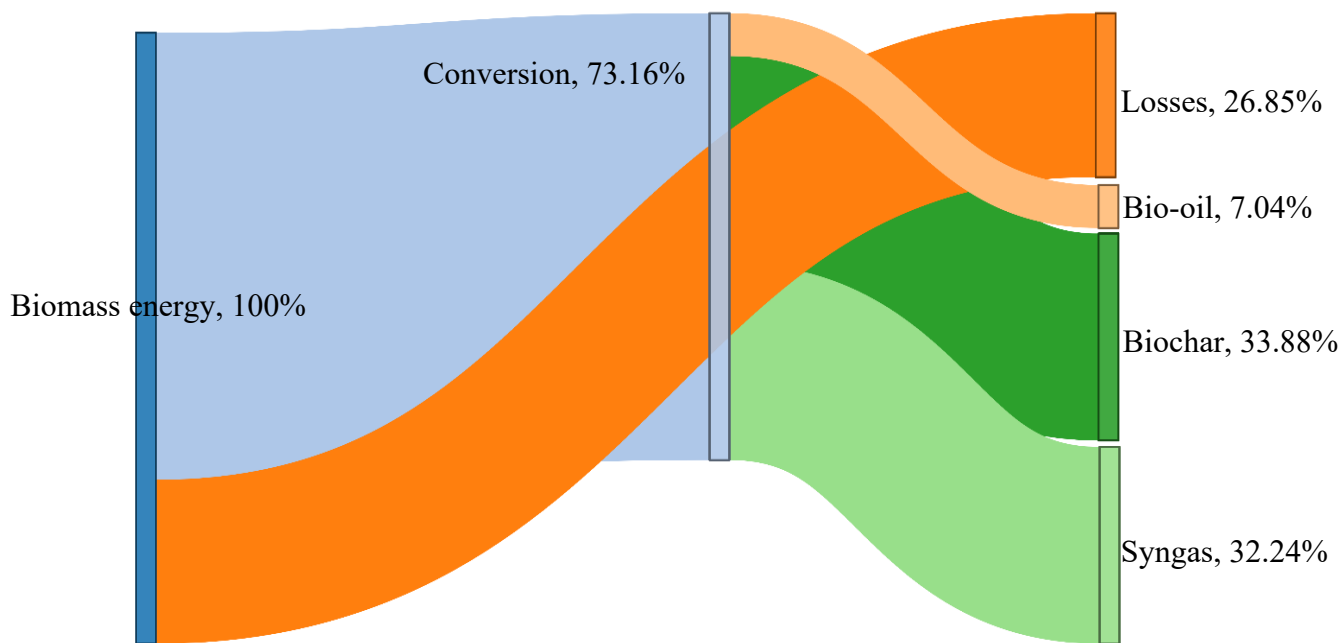


Figure 2.4. Average energy conversion and losses for the biomass conversion

The Sankey diagram in Figure 2.4 shows the average energy conversion and losses for the entire set of experiments. Almost 73% of the total energy available in the feedstock is converted to valorized products like bio-oil (7%), biochar (34%), and syngas (32%). Though bio-oil has a very high calorific value, because of the low yield during the reaction it contributes less to the energy balance. On average, almost 27% of the energy gets lost during the conversion in the aqueous phase and ambient condition compensation. A study by Santos et al. on wheat husk found yields of 8.5% bio-oil, 34.5% biochar, and 34.2% syngas; these results are comparable to ours [39].

2.6 Effect of reformer temperature

The catalytic cracking of the organic vapor with biochar is affected by the reforming temperature, producing bio-oil with different qualities and quantities. The quantitative and qualitative analyses

of biochar, bio-oil, and syngas were done at a fixed reactor temperature of 400 °C and variable reforming temperatures of 500, 600, and 700 °C.

2.6.1 Mass balance

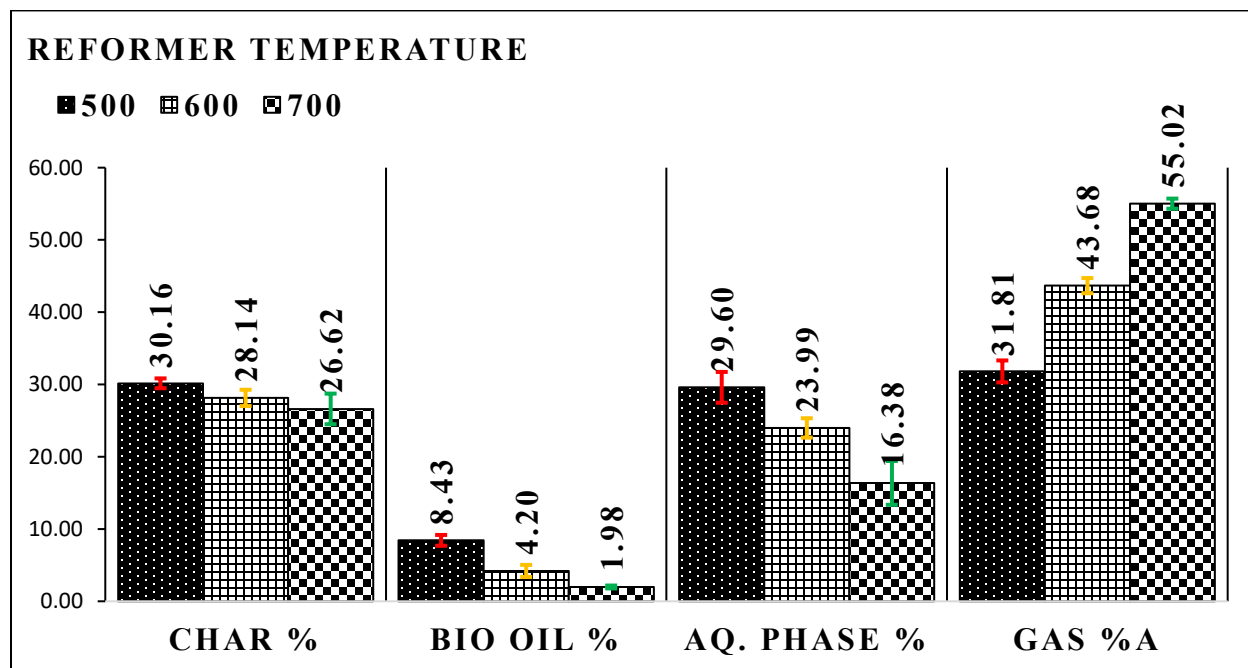


Figure 2.5. Product distribution at fixed reactor temperature of 400 °C and variable reformer temperatures

Figure 2.5 shows the distribution of biochar, bio-oil, aqueous phase, and syngas at a fixed reactor temperature of 400 °C and variable reformer temperatures of 500, 600, and 700 °C. Increasing the reformer temperature decreases the biochar, bio-oil, and aqueous phase, whereas gas yield increases with an increase in the reformer temperature. The increase in yield with an increase in reformer temperature was also observed by Neumann et al. [43]. The increasing trend in the total yield and decrease in biochar and bio-oil yields are addressed by the reactions shown in Table 2.4. The total biochar yield decreased from 30.16 wt. % at 500 °C to 26.62 wt. % at 700 °C. This decrease in the total solid yield is explained by the solid carbon in the char reacting with the moisture and oxygen available in the feed to form carbon monoxide, methane, and hydrogen; these

reactions are demonstrated in reactions II, III, and VI in Table 2.4. The total bio-oil yield decreased by almost 77% when the reforming temperature increased from 500 to 700 °C. The total bio-oil yield was 8.43 wt. % at 500 °C and decreased by almost 77% when the temperature increased to 700 °C (1.98 wt. %); this reduction in the bio-oil is a result of the catalytic cracking of the organic vapor to yield more permanent gases. The total aqueous phase yield reduced from 29.60 wt. % at 500 °C to 16.38 wt. % at 700 °C; this reduction is a result of the carbon monoxide reaction with the moisture in the feed to form carbon dioxide and hydrogen (forward water-gas shift reaction). Biochar, bio-oil, and aqueous phase yields were significantly affected by the increase in the reforming temperature. Yet the total syngas yield increased by almost 73% with an increase in reformer temperature from 500 to 700 °C. An increase in the total gas yield occurs at the expense of reducing bio-oil, biochar, and aqueous phase. Ahmad et al. did a similar study with residual sugarcane bagasse at reformer temperatures of 500 to 700 °C and reactor temperatures of 200 to 500 °C in three reactor temperature zones. The experiment showed a similar increase in gas yield and decreases in the biochar, bio-oil, and the aqueous phase with an increase in the reformer temperature [42].

Table 2.4. Post-reforming reactions

Reaction	Enthalpy	Reaction No.
$CO_2 + C \leftrightarrow 2CO$	+172	I
$C + H_2O \leftrightarrow CO + H_2$	+131	II
$C + 0.5 O_2 \leftrightarrow CO$	-111	III
$CH_4 + H_2O \leftrightarrow CO + 3H_2$	+206	IV
$CO + H_2O \leftrightarrow CO_2 + H_2$	-41.2	V
$C + 2H_2 \leftrightarrow CH_4$	-74.8	VI

2.6.2 Biochar characterization

An ultimate analysis of the biochar produced at different reforming temperatures was conducted and the results are shown in Table 2.5. The overall carbon content in the produced biochar remains around 65-66%. Hydrogen content ranges from 1.3-1.9%, and sulfur and nitrogen content remain almost constant. The char produced has a very low O/C ratio and an even lower H/C ratio, indicating the better stability of char. The higher heating value of the char produced at 500 °C was found to be 21.4 MJ/Kg and was minimally affected by variations in the reforming temperature. Santos et al. conducted experiments with wheat husk at an average reactor temperature of 430 °C and a reformer temperature of 600 °C; the biochar produced had an HHV of 28.4 MJ/kg [39]. A proximate analysis of the char samples was conducted; the total dry fixed carbon was highest for char produced at a reforming temperature of 600 °C and lowest for char produced at 700 °C. The total volatiles are in the range of 7 to 10 dry wt. %, whereas the total ash content is in the range of 23 to 29 dry wt. %.

Table 2.5. Properties of biochar at a fixed reactor and variable reformer temperatures

	Ultimate analysis (dry, ash-free basis) (wt. %)		
	Reforming temperature		
	500 °C	600 °C	700 °C
Carbon	65.6	64.9	66.1
Hydrogen	1.9	1.1	1.3
Nitrogen	0.8	0.8	0.8
Sulfur	0.2	0.2	0.2
Oxygen(a)	31.5	32.9	31.6
O/C	0.481	0.506	0.477
H/C	0.029	0.018	0.019
	Proximate analysis, (dry basis) (wt. %)		
Volatile	10.45	9.24	7.08
Ash	24.04	22.71	29.16
Fixed carbon	65.52	68.05	63.76
Moisture	1.66	1.56	2.05
HHV (MJ/kg)	21.4	20.2	20.9

(a) calculated by the difference

2.6.3 Bio-oil characterization

Ultimate, TAN, and viscosity analyses were done on the bio-oil produced at variable reforming temperatures, and the results are presented in Table 2.6. The total carbon and sulfur content in the bio-oil increases with an increase in reforming temperature; however, the total hydrogen and oxygen content in the bio-oil decreases with an increase in reforming temperature. The decrease in oxygen and hydrogen content is explained by the favorable reduction reaction at higher reforming temperatures. The total oxygen content in the bio-oil was 17.6% at 500 °C; with increasing reformer temperature, it decreased gradually and reached 11.7% at 700 °C. Neumann et al. experimented with digestate at a reactor temperature of 450 °C and variable reformer temperatures (no reforming, 500 °C reforming, and 750 °C reforming); the oxygen concentration (by difference) on a moisture ash-free basis was found to be relatively lower than that of the wheat straw pellets experimented on in this study. The lower oxygen content in the bio-oil ultimate analysis can be explained by the type of feedstock and the slight variation in experimental conditions [43]. The lowest (56.68 mg KOH/g) TAN was observed at a 700 °C reformer temperature and showed an increasing trend with the decrease in reformer temperature. The viscosity was lowest (35.16 mPas) at a 600 °C reformer temperature and highest at a 700 °C reformer temperature. The HHV of the bio-oil was greatest (35.2 MJ/kg) at 600 °C and lowest at a reformer temperature of 500 °C. Santosh et al. reported the HHV of bio-oil produced from wheat husks to be 26 MJ/kg [39], and in another experiment on digestate, Neumann et al. reported around 35±1 MJ/kg [43]. Elmously et al. experimented with spent coffee grounds at similar reactor and reformer temperatures and found a maximum HHV of 36.8 MJ/kg, comparable to the maximum found in this study [57].

Table 2.6. Ultimate analysis, HHV, TAN and viscosity of bio-oil produced at different reforming temperatures

Ultimate analysis (dry, ash-free basis) (wt. %)			
	Reforming temperature		
	500 °C	600 °C	700 °C
Carbon	71.6	76.5	78.3
Hydrogen	9.0	8.3	6.9
Nitrogen	0.8	0.8	0.8
Sulfur	0.3	0.4	0.6
Oxygen(a)	17.6	12.8	11.7
O/C	0.246	0.167	0.150
H/C	0.126	0.108	0.088
HHV (MJ/kg)	33.8	35.2	34.3
TAN (mg KOH/g)	116.32	105.36	56.68
Viscosity (mPas)	38.84	35.16	51.35

(a) calculated by the difference

The GC-MS analysis results of bio-oil produced from the fixed reactor and variable reforming temperatures are summarized in Table 2.7. An increase in reforming temperature leads to an increase in polyaromatic hydrocarbons (PAHs) and monoaromatic hydrocarbons (MAHs), whereas phenols and alcohols decreased. Surprisingly, the total oxygenated compound increased with an increase in reforming temperature, but it remained below 9% at all reforming temperatures. The reduction in phenol and the alcoholic compound is explained by the increase in secondary cracking and deoxygenation reactions at higher reforming temperatures, resulting in high aromatics.

Table 2.7. Summary of GC-MS analysis results at fixed reactor and different reforming temperatures

Compound	Reforming temperature		
	500 °C	600 °C	700 °C
MAHs	17.60	24.46	16.17
PAHs	2.24	11.48	44.75
FAMEs (fatty acid methyl esters)	10.03	3.50	1.83
N- compound	1.32	0.94	1.18

Compound	Reforming temperature		
	500 °C	600 °C	700 °C
O- compound	2.70	8.16	6.94
Phenols and alcohols	65.02	50.90	29.14
Acids	0.00	0.00	0.00
Alkanes	0.98	0.00	0.00
Chlorine compound	0.11	0.00	0.00
Total detection (%)	74.76	81.95	86.32

Table 2.8 shows the detailed elemental analysis of the same bio-oil samples. Bio-oil produced at a 500 °C reformer temperature has very high (almost 65%) phenol and alcohol content, which decreases by almost 55% to 29.14% at 700 °C. MAHs have a zigzag trend; the MAH was highest (24.46%) at a 600 °C reformer temperature and lowest (16.17%) at 700 °C, whereas PAHs have an increasing trend and were highest (44.75%) at 700 °C. Slight traces of alkenes and chlorine compounds were also detected at low reforming temperatures. Ahmad et al. found this same reduction of phenolic compounds at higher reforming temperatures in their work on residual sugarcane bagasse [42].

Table 2.8. Detailed GC-MS results with bio-oil produced at a variable reforming temperatures for agricultural residues

SN	Compound Name	Reformer temperature		
		500 °C	600 °C	700 °C
		%	%	%
1	1,4-Dihydronaphthalene	-	-	1.29
2	1H-Indene, 1-ethylidene-	-	2.14	-
3	1H-Indene, 1-methyl-	0.59	-	-
4	1H-Indene-1-one,2,3-dihydro	0.65	-	-
5	2-Cyclopenten-1-one, 2,3-dimethyl-	-	0.64	-
6	2-Cyclopenten-1-one, 2,3-dimethyl-	1.34	-	-
7	2-cyclopenten-1-one, 2,3-dimethyl-	0.33	-	0.39
8	2-Cyclopenten-1-one, 2-methyl-	1.54	0.76	0.42
9	2-Cyclopenten-1-one, 3-methyl-	0.86	-	0.41
10	2-Naphthalenol	-	0.44	0.32

SN	Compound Name	Reformer temperature		
		500 °C	600 °C	700 °C
		%	%	%
11	4H-Cyclopenta[def]phenanthrene	-	-	0.61
12	Acenaphthylene	-	0.76	3.67
13	Acetophenone	0.24	0.21	-
14	Anthracene, 9-methyl-	-	-	0.65
15	Azulene	1.62	-	-
16	Benzene, (1-methyl-2-cyclopropen-1-yl)-	-	1.96	-
17	Benzene, (1-methyl-2-cyclopropen-1-yl)-	-	1.21	0.76
18	Benzene, 1,2,3-trimethyl-	-	0.40	0.19
19	Benzene, 1-ethenyl-2-methyl-	-	-	0.64
20	Benzene, 1-ethyl-4-methoxy-	1.47	-	0.42
21	Benzene, 1-ethyl-4-methyl-	-	0.81	0.24
22	Benzene, 1-ethyl-4-methyl-	0.71	-	-
23	Benzene, cyclopropyl-	-	0.64	-
24	Benzene, 1-Methyl-1,2-propadienyl-	0.89	-	-
25	Benzocycloheptatriene	0.97	-	-
26	Benzofuran	0.22	-	1.26
27	Benzofuran, 2,3-dihydro	0.28	0.66	0.53
28	Benzofuran, 2,3-dihydro-	-	3.60	1.91
29	Benzofuran, 2-methyl-	-	1.11	0.30
30	Benzofuran, 2-methyl-	-	0.51	0.49
31	Benzofuran, 2-methyl-	-	0.31	0.60
32	Benzylidenemalonaldehide	-	0.45	-
33	Biphenyl	-	0.25	0.93
34	Cyclopentanone	0.59	0.21	0.09
35	Ethyl-2-benzofuran	1.07	-	-
36	Ethylbenzene	0.59	0.74	0.34
37	Fluoranthene	-	0.14	0.63
38	Fluoranthene	-	-	0.46
39	Fluorene	-	0.42	0.46
40	Fluorene	-	0.27	1.08
41	Fluorene	-	0.13	0.48
42	Indane	0.21	1.09	-
43	Indene	0.99	3.22	-
44	Indene	-	-	5.48
45	Naphthalene	-	3.37	12.42
46	Naphthalene, 1,3-dimethyl-	-	0.45	-
47	Naphthalene, 1,5-dimethyl-	-	-	0.41
48	Naphthalene, 1,6-dimethyl-	-	0.49	0.20
49	Naphthalene, 2,6-dimethyl-	-	-	0.42
50	Naphthalene, 2-ethenyl-	-	-	1.41
51	Naphthalene, 2-methyl-	-	-	3.72
52	Naphthalene, 2-methyl-	-	1.47	2.59
53	Naphthalene, 1-methyl-	0.68	-	-

SN	Compound Name	Reformer temperature		
		500 °C	600 °C	700 °C
		%	%	%
54	Phenanthrene	-	0.53	2.60
55	Phenanthrene	-	0.24	0.96
56	Phenol	14.43	12.40	9.97
57	Phenol, 2,3-dimethyl-	-	0.63	-
58	Phenol, 2,3-dimethyl-	-	0.44	-
59	Phenol, 2,4-dimethyl-	3.34	2.80	1.29
60	Phenol, 2,6-dimethyl-	0.67	-	0.23
61	Phenol, 2-ethyl-4-methyl	1.54	-	0.29
62	Phenol, 2-ethyl-5-methyl-	0.56	0.72	-
63	Phenol, 2-methyl-	7.10	6.38	3.28
64	Phenol, 3,4-dimethyl-	-	0.79	0.24
65	Phenol, 3-ethyl-	-	1.19	0.69
66	Phenol, 3-ethyl-5-methyl-	-	0.70	-
67	Phenol, 3-methyl-	13.47	-	-
68	Phenol, 4-(2-propenyl)-	-	0.44	-
69	Phenol, 4-ethyl-	4.66	2.50	0.36
70	Phenol, 4-ethyl-	0.90	0.76	1.27
71	Phenol, 4-methyl-	-	11.33	6.90
72	Phenol,3-5-dimethyl-	0.71	-	-
73	Phenol,4-(1-methylethyl)-	0.58	-	-
74	P-Xylene	1.83	1.87	
75	P-xylene	0.37	0.79	1.05
76	Pyrene	0.21	0.19	0.91
77	Pyridine	0.17	0.38	0.64
78	Pyridine, 2-Methyl-	0.25	0.39	0.38
79	Styrene	-	1.59	2.23
80	Toluene	2.19	2.31	1.91

2.6.4 Permanent gas composition and properties

Table 2.9 and Figure 2.6 show the comprehensive gas analysis for the experiments done at a fixed reactor temperature of 400 °C and reformer temperatures of 500, 600, and 700 °C. The HHV of the syngas produced ranges from almost 8 MJ/kg to 12 MJ/kg, showing the increasing trend with an increase in the reforming temperature; this HHV is slightly lower than Ahmad et al.'s coffee ground experiment with similar reactor and reformer temperatures (20.6 to 23.1 MJ/m³) [42]. The

total hydrogen concentration was lowest (21.01%) at 500 °C and highest (36.32% and 34.99%, respectively) at 600 °C and at 700 °C. This higher concentration of hydrogen is justified by the water-gas shift reaction and methane reforming reactions and explained by Elmously et al. in their study [42, 57]. Methane and carbon dioxide decrease with an increase in reformer temperature, while carbon monoxide increases. The increasing trend of hydrogen and decreasing trend of methane show the occurrence of the forward gas shift reaction. Following our comprehensive analysis, we found that the syngas produced contains ethane, ethene, ethylene, propane, and traces of benzene.

Table 2.9. Comprehensive permanent gas analysis at the fixed reactor and variable reformer temperatures

Gases	Reformer temperature		
	500 °C	600 °C	700 °C
Hydrogen	21.01	36.32	34.99
Methane	15.53	14.19	14.38
Carbon dioxide	39.97	28.86	23.24
Carbon monoxide	12.29	10.67	11.38
Ethane	2.02	1.19	0.69
Ethene	1.22	2.57	4.69
Ethylene	0.01	0.09	0.24
Propane	0.43	0.17	0.05
Benzene	0.11	0.23	0.38
HHV(MJ/kg)	8.16	11.38	11.84

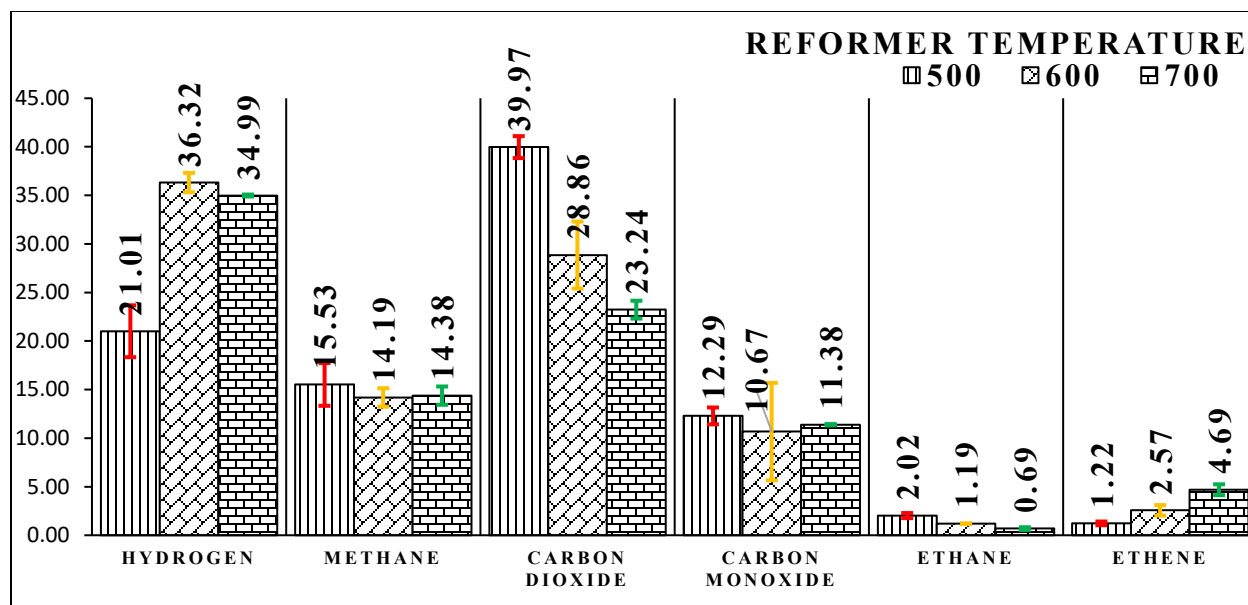


Figure 2.6. Major gas composition at a fixed reactor temperature

2.7 Effect of reactor temperature

The reactor temperature is another crucial parameter that can affect the quality and quantity of final products (bio-oil, biochar, syngas, and aqueous phase). The effect of reactor temperature at fixed reformer temperatures of 600 °C and 700 °C was studied and is discussed in the following sections. The reformer temperature was set to 600 °C and the reactor temperature varied from 400 to 500 °C; and the reformer temperature was set to 700 °C and the reactor temperature varied from 400 to 550 °C with increments of 50 °C on each set of experiments.

2.7.1 Mass balance

Figure 2.7 shows the proportions of biochar, bio-oil, syngas, and aqueous phases produced at different reactor temperatures and a fixed reforming temperature of 600 °C. Char yield has an overall decreasing trend with an increase in reactor temperature. The highest biochar yield (28.14 wt. %) was found at a 400 °C reactor temperature, whereas the lowest yield (27.37 wt. %) was found at a 700 °C reactor temperature. The bio-oil yield decreased from 4.20 wt. % to 2.94 wt. %

with an increase in reactor temperature from 400 to 500 °C. These results are comparable with previous experiments on wheat husk [39], woody biomass [45], residual sugarcane bagasse [42], and digestate [43]. Jäger et al. performed experiments with woody biomass at a reactor temperature of 400 °C and a reformer temperature of 600 °C and obtained a total bio-oil yield in the range of 3 to 4 wt. % [45]. Gill et al. experimented with softwood pellets at 450 °C reactor and 600 °C reformer temperatures; the resulting mass balance showed 4.16 wt. % bio-oil, 17.48 wt. % biochar, 18.16 wt. % aqueous phase, and 60.2% syngas [58]. At a higher reactor temperature, the pyrolysis vapor cracks along with the expense of bio-oil and biochar to get high syngas yield.

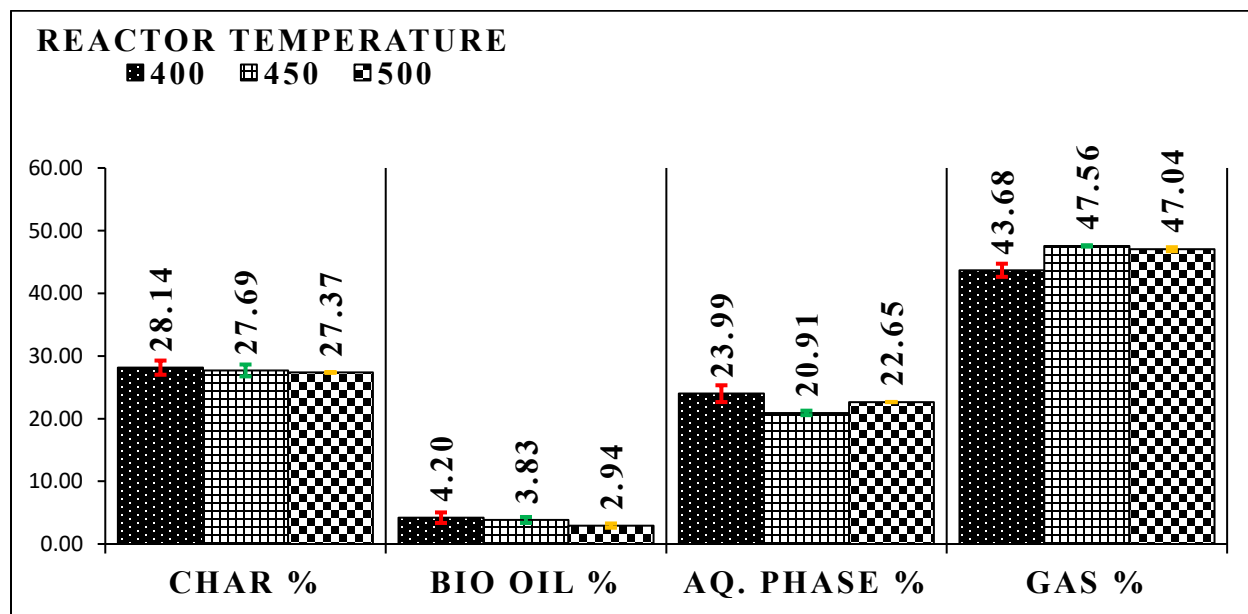


Figure 2.7. Mass balance at a fixed reforming temperature of 600 °C

Figure 2.8 shows the mass balance for the experiment performed at a reforming temperature of 700 °C. The total aqueous phase and total syngas yield do not show a clear trend, but the yield is within $\pm 2\%$. The total bio-oil yield showed an increasing trend; it reached a maximum value of 2.30% at a 500 °C reactor temperature and a minimum value at 550 °C. The total char yield is unaffected by variations in reactor temperature at a high reforming temperature of 700 °C, and most char mass is converted into permanent gases via the catalytic reforming reactions depicted in

Table 2.4. The higher fractions of gaseous product were also explained in Ahmad et al.'s experimental work on residual sugarcane bagasse [42]. The authors experimented at a fixed reformer temperature of 700 °C, and a total syngas yield was reported at 58.2 wt. %, comparable to the yield obtained from the current study using wheat straw pellets.

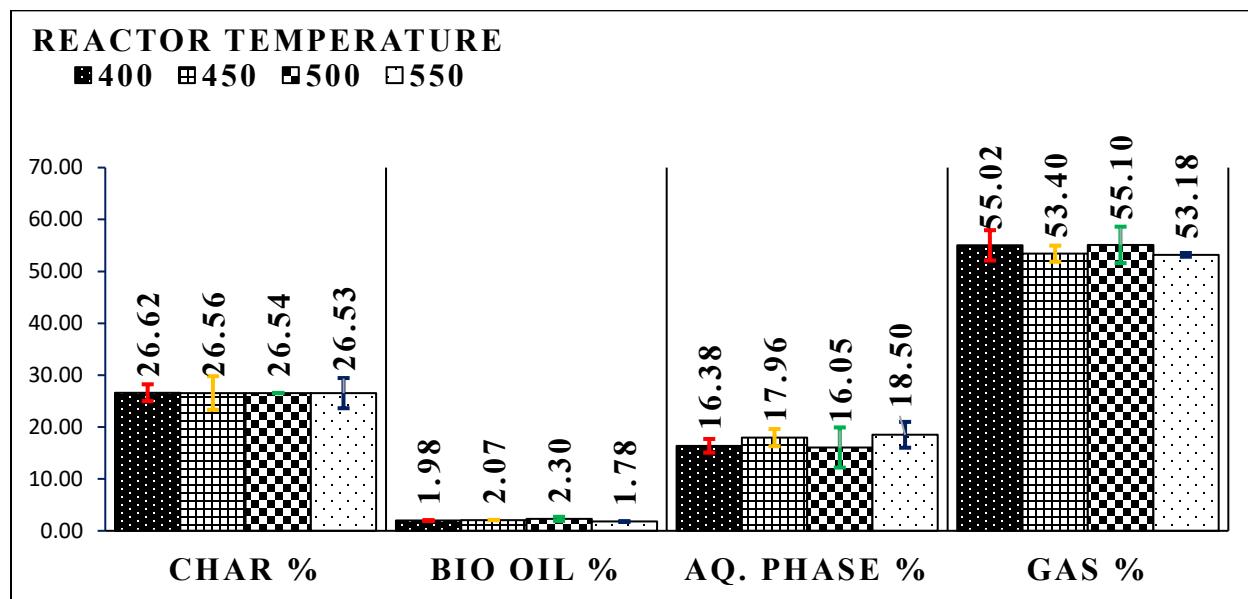


Figure 2.8. Mass balance at a fixed reforming temperature of 700 °C

2.7.2 Biochar characterization

Char collected at a fixed reforming temperature of 600 °C was subjected to an ultimate analysis, and the results are summarized in Table 2.10. The total carbon content in the biochar was found to be 65.2% at a 500 °C reactor temperature, and it was lowest at 450 °C. The total nitrogen and sulfur content in the biochar remain almost constant at 0.8 and 0.2%, respectively, irrespective of the variation in reactor temperature. The O/C and H/C ratios are in the range of 0.5 and 0.01, respectively, which indicates the excellent stability of the char. The HHV of the biochar produced is in the range of 19 to 20 MJ/kg. This HHV is lower the value reported by Gill et al. (32.57 MJ/kg) from their experimental work on softwood pellets at 450 (reactor) and 600 °C (reformer) temperatures [58]. The difference in feedstock composition can explain this difference in HHV. In

Ahmad et al.'s experiment with residual sugarcane bagasse at a reactor temperature of 450 °C and a reformer temperature of 700 °C, the HHV obtained for the solid (biochar) product was 21.2 MJ/kg; this value is comparable to that of the biochar obtained in this study [42]. Proximate analysis shows that the total volatiles in the char produced are in the range of almost 7 to 9 dry wt. %, ash in the range of 20 to 29 dry wt. %, and total fixed carbon in the range of 63 to 71 dry wt. %. The moisture content in the char produced is lower than 2 wt. % in all three experiments.

Table 2.10. Biochar characterization for a fixed reforming temperature of 600 °C

Ultimate analysis (dry, ash-free basis) (wt. %)			
	Reactor temperature		
	400 °C	450 °C	500 °C
Nitrogen	0.8	0.8	0.8
Carbon	64.9	63.1	65.2
Hydrogen	1.1	1.0	1.2
Sulphur	0.2	0.2	0.2
Oxygen(a)	32.9	34.9	32.6
O/C	0.5065	0.5532	0.5006
H/C	0.0177	0.0155	0.0185
Proximate analysis (dry basis) (wt. %)			
Volatile	9.24	7.08	8.12
Ash	22.71	29.16	20.84
Fixed carbon	68.05	63.76	71.04
Moisture	1.56	2.05	1.75
HHV MJ/kg	20.2	19.0	20.2

(a) calculated by the difference

The ultimate and proximate analyses of the biochar produced at a fixed reformer temperature of 700 °C and variable reactor temperatures of 400 to 550 °C show similar results to those in Table 2.10. The highest HHV obtained at a 700 °C reformer temperature was 20.9 MJ/kg at a 400 °C reactor temperature.

2.7.3 Bio-oil characterization

Ultimate analysis of the bio-oil produced showed that the O/C and H/C ratios are very low, indicating good bio-oil stability. The variations in TAN, viscosity, and the HHV of bio-oil at

variable reactor temperatures (400 to 550 °C) and fixed reactor temperatures of 600 and 700 °C are shown in Table 2.11. Experiments at fixed reformer temperatures of 600 and 700 °C showed a decrease in TAN and viscosity with an increase in reactor temperature. The lowest TAN (7.3 mg KOH/g) and viscosity (3.9 mPas) were found for the bio-oil produced at 550 °C (reactor) and 700 °C (reformer) temperatures. For almost the same reactor and reformer temperature conditions, experiments with sugarcane bagasse yielded bio-oil with 16.1 mg KOH/g TAN and with digestate, bio-oil with 5.1 mg KOH/g TAN and 40 mPas viscosity [42]. The highest HHV (36.8 MJ/kg) for the bio-oil produced was observed at 500 °C (reactor) and 700 °C (reformer) temperatures; however, at a high reforming temperature, the HHV remains almost stable at around 35 MJ/kg irrespective of the reactor temperature. This HHV was higher than that in the experiment conducted on sugarcane bagasse by Ahmad et al. [42].

Table 2.11. Ultimate analysis, TAN, viscosity, and HHV of bio-oil at fixed reformer temperatures of 600 and 700 °C

Ultimate analysis (dry, ash-free basis) (wt. %)							
Reactor Temperature	Reformer temperature						
	600 °C			700 °C			
	400 °C	450 °C	500 °C	400 °C	450 °C	500 °C	550 °C
Carbon	76.5	78.4	78.5	78.3	82.4	81.0	83.5
Hydrogen	8.3	8.3	6.9	6.9	6.3	8.0	6.3
Nitrogen	2.1	1.6	2.7	2.5	2.2	2.3	2.2
Sulfur	0.4	0.2	0.6	0.6	0.4	0.3	0.3
Oxygen(a)	12.8	11.4	11.3	11.7	8.8	8.4	7.7
O/C	0.167	0.146	0.144	0.150	0.107	0.104	0.092
H/C	0.108	0.106	0.089	0.088	0.076	0.099	0.076
TAN (mg KOH/g)	35.16	33.98	30.36	51.4	31.4	12.9	7.3
Viscosity (mPas.)	105.36	70.26	41.97	56.7	4.5	5.5	3.9
HHV (MJ/kg)	35.2	36.0	34.5	34.3	35.2	36.8	35.8

(a) calculated by the difference

The compounds detected by GC-MS are categorized into six major categories and presented in Figure 2.9. With an increase in the reactor temperature, phenols/alcohol and FAMES showed a decreasing trend, whereas PAHs showed an increasing trend. The reactor temperature has a small effect on the concentration of the oxygen compound in the samples, which fluctuates between 8.16 to 8.53% at 400 and 500 °C, respectively. The amounts of MAH and N-compounds were highest at 450 °C (at 27.23 and 1.75%, respectively), and the lowest concentrations were obtained at a 500 °C reactor temperature. Phenols and their derivatives undergo deoxygenation and secondary cracking reaction to yield higher aromatics; hence, at a higher temperature, the ratio of PAHs and MAHs to phenol/alcohol increases.

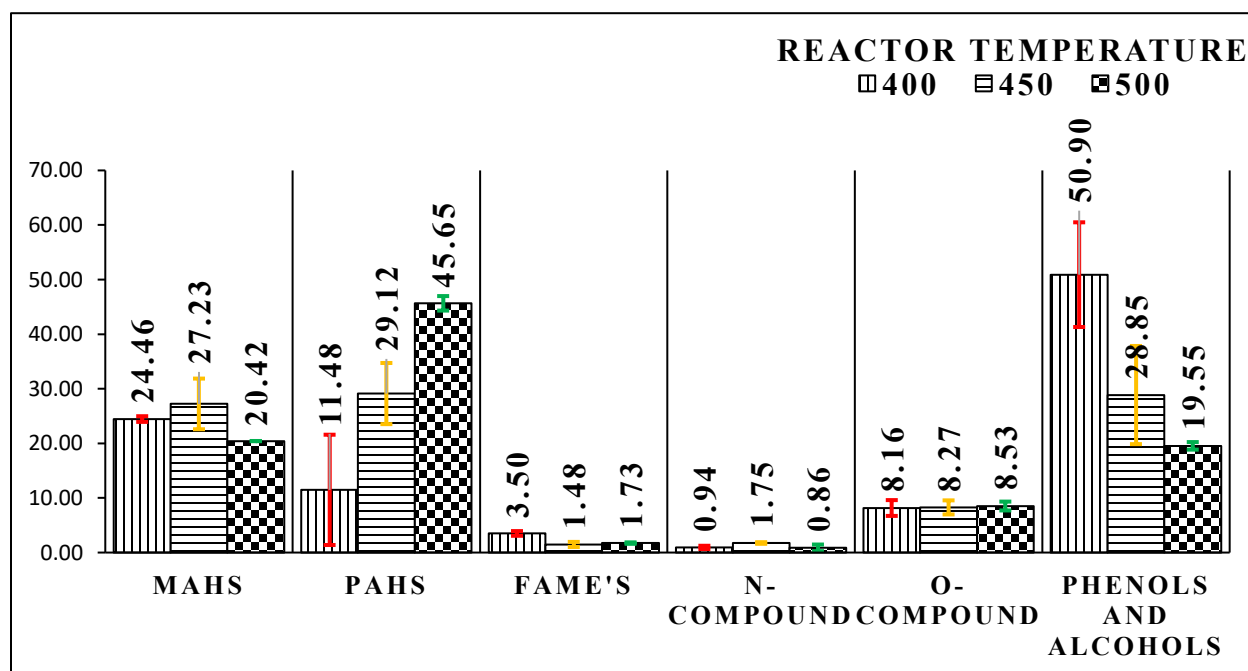


Figure 2.9. GC-MS analysis of bio-oil produced at a fixed reformer temperature of 600 °C

A detailed GC-MS analysis is presented in Table 2.12. The % column in the table represents the total area each compound covers in the GC-MS chart. At a 400 °C reactor temperature, phenol and its derivatives covered almost 31% of the total chart area, followed by PAHs like naphthalene and

its derivatives and MAHs like indene and its derivatives. At a 450 °C reactor temperature, the top 3 compounds are phenol, naphthalene derivative, and p-xylene at 12.1, 10.6, and 10.6%. Similarly, at a 500 °C reforming temperature, the top 3 compounds are phenol, phenanthrene, and anthracene derivatives at 11.2, 9.9, and 9.9%. The total compound detection percentages for 400, 450, and 500 °C are 74.76, 81.95, and 86.32%, respectively, which are later normalized to 100 to be presented in Table 2.12.

Table 2.12. GC-MS analysis of bio-oil produced at a fixed reformer temperature of 600 °C

SN	Compound name	Reactor temperature		
		400 °C %	450 °C %	500 °C %
1	1,4-Dihydronaphthalene	-	3.00	-
2	1H-Indene, 1-ethylidene-	2.14	-	-
3	1H-Indene, 1-methyl-	-	-	2.85
4	1H-Phenalene	-	-	0.48
5	2-Cyclopenten-1-one, 2,3-dimethyl-	0.64	0.34	-
6	2-Cyclopenten-1-one, 2-methyl-	0.76	0.41	-
7	2-Cyclopenten-1-one, 2-methyl-	-	-	0.38
8	2-Naphthalenol	0.44	0.40	-
9	4-(3-Methoxyphenyl)propylcyanide	-	0.56	-
10	Acenaphthylene	0.76	1.37	1.21
11	Acetic acid, 4-methylphenyl ester	-	1.11	1.24
12	Acetic acid, phenyl ester	-	1.78	1.57
13	Anthracene, 2-methyl-	-	-	9.87
14	Anthracene, 9-methyl-	-	-	0.51
15	Benzene, (1-methyl-2-cyclopropen-1-yl)	1.21	1.45	1.40
16	Benzene, (1-methyl-2-cyclopropen-1-yl)-	1.96	-	-
17	Benzene, 1,2,3-trimethyl-	0.40	-	0.39
18	Benzene, 1,2,4-trimethyl-	-	0.43	-
19	Benzene, 1-ethyl-4-methyl-	0.81	0.80	0.75
20	Benzene, cyclopropyl-	0.64	0.93	0.85
21	Benzofuran, 2,3-dihydro-	0.66	0.72	0.72
22	Benzofuran, 2,3-dihydro-	3.60	4.65	4.19
23	Benzofuran, 2-methyl-	0.31	0.44	0.41
24	Benzofuran, 2-methyl-	0.51	0.68	0.64
25	Benzofuran, 2-methyl-	0.34	0.49	0.46
26	Benzofuran, 2-methyl-	1.11	0.88	0.99
27	Benzylidenemalonaldehide	0.45	-	-

SN	Compound name	Reactor temperature		
		400 °C	450 °C	500 °C
		%	%	%
28	Biphenyl	0.25	0.40	0.36
29	Biphenyl	-	-	0.56
30	Ethylbenzene	0.74	0.83	0.72
31	Fluorene	0.28	0.37	0.42
32	Fluorene	0.27	0.54	0.23
33	Fluorene	0.42	0.14	0.53
34	Indane	1.09	1.73	1.64
35	Indene	3.22	4.38	4.07
36	Naphthalene	3.37	4.88	9.87
37	Naphthalene, 1,3-dimethyl-	0.45	10.60	0.62
38	Naphthalene, 1,6-dimethyl-	0.49	-	0.29
39	Naphthalene, 2,3-dimethyl-	-	0.62	0.58
40	Naphthalene, 2-methyl-	1.47	2.73	2.63
41	Naphthalene, 2-methyl-	-	2.02	1.89
42	Phenanthrene	0.53	0.92	2.63
43	Phenanthrene	0.24	0.29	9.90
44	Phenol	12.40	12.06	11.23
45	Phenol, 2,3-dimethyl-	0.44	0.57	0.32
46	Phenol, 2,3-dimethyl-	0.63	-	0.54
47	Phenol, 2,4-dimethyl-	2.80	2.38	2.28
48	Phenol, 2-ethyl-4-methyl-	-	-	0.52
49	Phenol, 2-ethyl-5-methyl-	0.72	0.54	-
50	Phenol, 2-methyl-	6.38	6.16	0.58
51	Phenol, 3,4-dimethyl-	0.79	0.34	0.62
52	Phenol, 3,4-dimethyl-	-	0.67	-
53	Phenol, 3-ethyl-	1.19	-	-
54	Phenol, 3-ethyl-, acetate	-	-	0.50
55	Phenol, 3-ethyl-5-methyl-	0.70	-	-
56	Phenol, 4-(2-propenyl)-	0.44	-	-
57	Phenol, 4-ethyl-	0.76	0.84	0.78
58	Phenol, 4-ethyl-	2.50	2.06	0.78
59	Phenol, 4-methyl-	11.33	2.40	0.20
60	p-Xylene	1.87	10.60	1.72
61	p-Xylene	0.79	0.52	0.46
62	Pyridine	0.38	0.45	0.41
63	Pyridine, 2-methyl-	0.39	0.48	0.41
64	Pyrrole	-	0.23	-
65	Styrene	1.59	1.68	1.48
66	Toluene	2.31	2.38	1.99

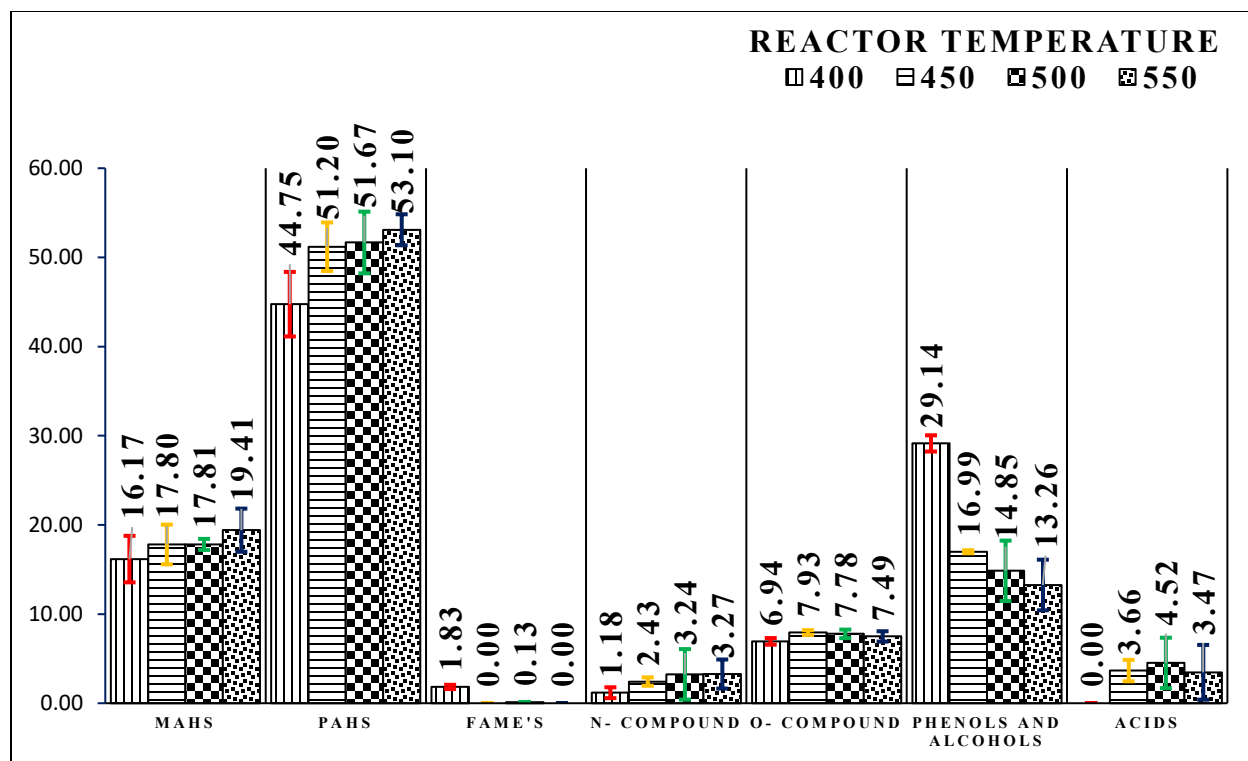


Figure 2.10. GC-MS analysis of bio-oil produced at a fixed reformer temperature of 700 °C

All the compounds detected in the GC-MS analysis were divided into seven major categories and are presented in Figure 2.10. With an increase in reactor temperature, the number of PAHs shows an overall increasing trend; however, it fluctuates in the 52±2% range from 450 °C onwards. The highest MAHs (23.16%) were detected at a reactor temperature of 400 °C and the lowest (17.18%) at 450 °C. N-compounds increase as the reactor temperature increases whereas O-compounds remain almost constant at 7%. 29.14% phenols/alcohols were observed at a 400 °C reactor temperature; after that, they decrease with an increase in reactor temperature and reach their lowest value (13.26%) at 550 °C. Some traces of FAMEs were observed at a low reactor temperature and acidic compounds started to appear when the reactor temperature exceeded 450 °C. A similar analysis was conducted by Ouadi et al. on municipal solid waste at a reactor temperature of 450 °C and a reformer temperature of 700 °C [48]. GC-MS analysis on the bio-oil produced from MSW showed a very high proportion of PAHs (49.6%) and MAHs (29.3%), and lower amounts

of other constituents like phenols (7.1%), FAMEs (3.3%), other alkanes, alkenes, O-compounds, and N-compounds.

2.7.4 Permanent gas composition and properties

Comprehensive gas analysis was done for the samples collected for a fixed reformer temperature of 600 °C and variable reactor temperatures of 400 to 500 °C at intervals of 50 °C, and the results are displayed in Table 2.13. The higher heating value of syngas produced is greatest (12.81 MJ/kg) at 450 °C and lowest (11.29 MJ/kg) at 500 °C. The total hydrogen yield remained almost unaffected with an increase in the reactor temperature and was in the range of 36%. In contrast, carbon monoxide yield increased sharply and reached 23.68% at 450 °C from 10.67% at 400 °C. Both methane and carbon dioxide show a decreasing trend with an increase in reactor temperature, which is defined by forward gas shift reactions. The forward gas shift reaction yields high amounts of hydrogen and carbon monoxide at high temperatures. Traces of ethane, ethene, ethylene, and propane were detected in the samples through comprehensive analysis. Jäger et al. also found high yields of hydrogen concentration at a high reforming temperature in their experiments [45]. They reported 33-36% hydrogen in syngas at a reactor temperature of 400 and a reformer temperature of 600 °C for woody feedstock. Santos et al. experimented with wheat husk at a reformer temperature of 600 °C (reactor average 430 °C), and the hydrogen volume proportion obtained (19.4 vol. %) was significantly below our results [39].

Table 2.13. Comprehensive gas analysis at a fixed reformer temperature of 600 °C

	Reactor temperature		
	400 °C	450 °C	500 °C
Hydrogen	36.32	35.74	35.03
Methane	14.19	13.22	11.47
Carbon dioxide	28.86	25.99	22.91
Carbon monoxide	10.67	23.68	25.91
Ethane	1.19	1.19	0.95

	Reactor temperature		
	400 °C	450 °C	500 °C
Ethene	2.57	2.60	1.93
Ethylene	0.09	0.07	0.06
Propane	0.17	0.15	0.12
Benzene	0.23	0.05	0.17
HHV(MJ/Kg)	11.38	12.81	11.29

At a fixed reformer temperature of 700 °C, the gas composition was similar.

The greatest hydrogen yield was obtained at a reactor temperature of 400 and lowest at 450 °C. The HHV of the syngas ranged from 11.84 MJ/kg to 12.54 MJ/kg. Neumann et al. experimented on digestate at 700 °C reformer and 450 °C reactor temperatures and reported 37% hydrogen in the syngas mixture, comparable with the values we obtained in our wheat straw pellets experiments [44].

2.8 Conclusion

The experimental thermo-catalytic reforming of agricultural residue (wheat straw) produces syngas with a very high concentration of hydrogen, superior quality bio-oil, and biochar with excellent stability. The bio-oil has a very low TAN (7.3 mg KOH/g) and low viscosity (3.9 mPas) at a reformer temperature of 700 °C and a reactor temperature of 550 °C compared to the bio-oil produced from the fast pyrolysis process. At a reforming temperature of 700 °C, PAHs and MAHs obtained from the experiment were more than 62% of the total bio-oil yield. The total oxygen compound in the bio-oil was below 9% in all bio-oil samples, showing the superior quality of the bio-oil. Additionally, the bio-oil has a very high HHV in the range of 35 MJ/kg, an O/C ratio in the range of 0.1, and an H/C ratio in the range of 0.01; this further strengthens the superiority of the bio-oil produced from the wheat straw. The syngas produced has a very high hydrogen content (up to 36.32 vol. % at a reactor temperature of 450 °C and reformer temperature of 600 °C). The syngas also has up to 15.53 vol. % methane, a minimum of 18 vol. % carbon dioxide, and up to

30.94 vol. % carbon monoxide. All other constituents of syngas were less than 5% on a volume basis. Low O/C and high H/C ratio of biochar showed it can be used as a fuel for thermal energy generation purpose. Furthermore because of its good porosity, biochar can be used for adsorption applications, as a catalyst and for soil enrichment purposes. High quality bio-oil can be directly mixed with the currently used liquid fuel after minimum upgradation and high hydrogen syngas can be utilized as a source of hydrogen or can be utilized to produce methanol by utilizing hydrogen and carbon monoxide produced.

Chapter 3: Parametric optimization of thermo-catalytic reforming of softwood pellets to produce biofuels

3.1 Introduction

Canada has committed to reduce its 2005-level greenhouse gas (GHG) emissions by 30% by 2030. Most GHG emissions come from the oil and gas sector, the transportation sector, and building use (heating and cooling), at 26%, 25%, and 13%, respectively [59]. Despite its commitment, Canada currently produces only 8% of its total primary energy from hydro and other renewables, i.e., wind, solar, wood/wood waste, biofuels, and municipal waste. The majority of this 8% is from hydro (67.1%) and solid biomass (23.1%) [60]. Canada has large forest and agricultural biomass potential. Availability of municipal solid waste (MSW) is also growing steadily which is also a biomass resource. All of these can be converted to energy and help in reduction of GHG emissions.

Biomass residues and organic wastes can be converted into various forms of energy through different biochemical and thermochemical processes [61]. The biochemical processes are in various stages of research and development; however, the thermochemical approach is being preferred because it has a faster processing time than the biochemical process. Thermochemical methods such as combustion, gasification, liquefaction, hydrogenation, and pyrolysis are used to convert biomass into valorized products [62].

Pyrolysis is the primary method of converting biomass into biofuels because its technology is the most advanced [63] and takes place in absence of oxygen. There are three main types of pyrolysis – fast, intermediate, and slow – based on temperature, heating rate, and vapor residence time. Each can be categorized further by the product distribution in the solid, permanent gas, and liquid (aqueous and organic) yields [43]. Fast pyrolysis is characterized by a rapid heating rate, short gas residence time (because of the fast char removal process), and the rapid disruption of the chemical

reaction that occurs by quenching. These factors result in a high liquid condensate with a significant amount of water [64]. The low reaction temperature and low heating rate in the slow pyrolysis process leads to a large amount of coke formation [65]. In intermediate pyrolysis, slow heating and long vapor residence time promote secondary cracking reactions that increase both char and hydrogen-rich permanent gas and improve bio-oil quality [64].

Though fast pyrolysis is the most cost-efficient route to convert biomass into liquid fuel, but there are challenges because of the diverse nature of the components in the final product. Because of shortcomings like a short lifetime (aging), high viscosity, and corrosivity, the product (bio-oil) needs to be upgraded so that it can be used directly in existing infrastructure [22, 66]. To overcome these issues, Fraunhofer UMSICHT introduced thermo-catalytic reforming technology (TCR[©]), which involves intermediate pyrolysis of the feedstock in an auger reactor followed by a post-reforming reaction. TCR[©] yields solid biochar, hydrogen-rich syngas, and bio-oil with excellent physical and chemical qualities [43, 54]. The low oxygen content and the high energy density of TCR[©] bio-oil make it superior to any other pyrolytic oil. Additionally, it is easier to transport and store because of its high energy density [48]. Even though this technology is suitable for feedstock with a moisture content up to 70 wt. %, the moisture content needs to be reduced. Any feedstock with an HHV of 8 MJ/kg and a moisture content of less than 20 wt. % can be processed by TCR[©] technology [43] but the feedstocks needs to be converted to pellets. The following feedstocks pellets have been tested in a lab-scale 2 kg/h TCR[©] plant: woody biomass [24], sugarcane bagasse [25], municipal solid waste (MSW) [48], sewage sludge [67], pulp rejects [47], agricultural residue (wheat husk) [39], spent coffee grounds [68], co-form rejects [46], digestates [43], and market waste [69].

Experiment with MSW have yielded 6%, 31%, and 44% bio-oil, char, and syngas, respectively, at a pyrolysis temperature of 450 °C and a reforming temperature of 700 °C [48]. The produced bio-oil has a total acid number (TAN) of 2.9 mg KOH/g and a kinematic viscosity of 6.5 cSt. An analysis of bio-oil shows a high quantity of polyaromatic hydrocarbons (PAHs) and monoaromatic hydrocarbons (MAHs) (49.6% and 29.3% of the total composition) [48]. This oil composition is suitable to blend with biodiesel. Because of its low oxygen content, it is favorable to use in diesel engines (i.e., it has low NO_x emissions). A high hydrogen content (36%) was observed in syngas due to the water-gas shift reaction [48].

Neumann et al. performed experiment with anaerobic digestate feedstock and the results of no reforming, reforming at 500 °C, and reforming at 750 °C with a fixed reactor temperature of 450 °C were compared. The permanent gas yield from this set of experiments shows an increasing trend with an increase in the reforming temperature. The amount of char produced decreases with an increase in the post-reforming temperature, and bio-oil yield was maximum at a 500 °C reformer temperature. Neumann et al. concluded that with an increase in the reforming temperature, the amount of hydrogen increases significantly, from 7% with no reforming to 37% with reforming at 750 °C. Despite the lower yield at a higher reforming temperature, the bio-oil produced at 750 °C has very low oxygen content (7%), a low TAN (5.1), and a viscosity of 40 cSt [43].

Jäger et al. tested three types of agricultural woody biomass (olive, evergreen oak, vine shoots) in the TCR[®] unit at a fixed reactor temperature of 400 °C and a post-reforming temperature of 600 °C [45]. Feedstock type has little or no effect on the total bio-oil yield, whereas total char yield was highest (23.4%) for vine shoots and lowest for olive wood (20.1%). At a reforming temperature of 600 °C, the total hydrogen concentration in syngas for three kinds of wooden feedstocks ranged from 33 to 36 vol% and the HHV ranged from 14.6 to 14.9 MJ/kg [45].

Canada has a vast forest area, an estimated 9% of the world's forests, and so woody biomass was chosen as the feedstock for this study. This paper investigates the thermo-catalytic reforming of woody biomass in a lab-scale 2 kg/h TCR[®] plant to produce biofuels. The specific objectives include the study of the dependency of operating conditions on the quality and quantity of the TCR[®] products. The first part of the study focused on the effect of reformer temperature at a fixed reactor temperature and the second part on the effect of reactor temperature at a fixed reformer temperature. The CHNS, viscosity, TAN, pH, and composition (GC-MS) in the produced bio-oil were analyzed. Char was subjected to CHNS analysis and pH, whereas syngas was analyzed through gas chromatography. Different experimental conditions were compared to determine the optimal operating conditions to produce bio-oil.

3.2 Material and methods

3.2.1 Feedstock characterization

The feedstock for the TCR[®] should be pellets or granules. The granules should be between 3 and 20 mm and pellets should be 10-25 mm long and 6 mm in diameter. Smaller particles may create difficulty during conveyance and especially in TCR[®] units which are of laboratory or pilot scale. Large particles are not desirable either because of the chances of blockage in the auger reactor and limitations on heat transfer to the biomass particle. The water content of the feedstock used in the TCR[®] for better efficiency of the equipment should be between 5 and 25%. For this study, softwood pellets were supplied by Vanderwell Contractors in Slave Lake, Alberta (illustrated in Figure 3.1).

Table 3.1. gives the ultimate and proximate analysis results of the feedstock used in the experiments. A Carlo Erba EA 1108 Elemental Analyzer was used. Carbon, hydrogen, nitrogen, and sulfur were measured using ASTM E777[51], ASTM E777 [51], ASTM E 778 [52], and

ASTM E775[53], respectively, and oxygen was measured by difference. The same method was used for the biochar produced in the experiments. The proximate analysis was done with a LECO TGA 701 following the ASTM D7582 standard[50]. The HHV of the feedstock was calculated using the following equation from literature [70]:

$$\text{HHV} \left(\frac{\text{MJ}}{\text{kg}} \right) = 0.3491 (C) + 1.1783(H) + 0.1005(S) - 0.1034(O) - 0.0151(N) - 0.0211(A)$$

where C, H, S, O, N, A represent the values of carbon, hydrogen, sulfur, oxygen, nitrogen, and ash.



Figure 3.1. Softwood pellets

The proximate analysis of the feedstock showed 77.20% volatiles, 16.19% fixed carbon, 5.46% moisture content, and 1.15% ash content. The ultimate analysis showed a high concentration of carbon at 48.27%, followed by oxygen at 45.64%, hydrogen at 6.09%, and nitrogen at <0.1%. The results were cross-validated with the results of a study by Jager et al. for a similar feedstock [24].

Table 3.1: Ultimate and proximate analysis of softwood pellets

Ultimate analysis (dry basis) (wt. %)	
Carbon	48.27
Hydrogen	6.09
Nitrogen	<0.1
Sulfur	0
Oxygen (a)	45.64

Proximate analysis (wt. %)	
Volatiles	77.20
Fixed carbon	16.19
Ash	1.15
Moisture	5.46
HHV (MJ/kg)	19.31

3.2.2 Experimental setup

The experimental setup consists of 3 electric motors, a feed hopper (1), feeding screw (2), auger reactor (3), fixed bed reformer (4), condensers (5), bio-oil container (6), gas wash bottle (7), filters (8), gas analyzer (9), and gas vent, as shown in Figure 2.3 in chapter 2. The top hopper's designed capacity is 6 kg, and it is physically attached to the top of the feeding screw conveyor. The feeding screw is driven by a pulsating electric motor, which ensures there is no blockage and maintains the continuous flow of feed to the auger reactor. The auger reactor, where intermediate pyrolysis takes place, consists of three different heating zones. The first is maintained at a temperature lower than pyrolysis temperature to clear out moisture and light volatiles from the feed and raise the feed temperature close to the required pyrolysis temperature. The second and third zones act as pyrolysis zones, with temperature ranges from 400 °C - 500 °C. Most of the volatiles and oxygenates escape, leaving the biochar behind. The biochar and all the vapors produced during pyrolysis travel to the reformer, which is generally maintained at a temperature of 500 °C to 700 °C, and also acts as a char collection unit. The reformer unit design is such that the vapors produced during pyrolysis make good contact with the char bed before exiting the reformer. The char itself acts as a catalyst for the catalytic reforming of the vapors. Hot reformed gas passes through two water-cooled condensation units in series maintained at -5 °C to -10 °C. The condensate consists of an organic liquid fraction, and the aqueous phase is collected in a glass bottle. The non-condensable fraction of cooled gases passes through the gas wash bottle filled with the aqueous

phase from the previous experiment (or ethanol from the first experiment) to capture aerosol present in the non-condensable gases. The aerosol-free gases then pass through two filters connected in series. Finally, the clean gas goes to the online gas analyzer. At the end of the experiment, after the reactor and reformer have cooled, the biochar is collected from the bottom of the reformer. For the first experiment, the reformer will not have a char bed to start. For successive experiments, char from each previous experiment (those with the same reformer temperature) can be used to prefill the reformer before the experiment is started. The reactor and reformer temperatures used in the experiments are shown in Table 3.2.

Table 3.2. Operating conditions

Feedstock	Reactor temperature (°C)	Reformer temperature (°C)
Softwood pellets	400 °C, 450 °C, 500 °C, 550 °C, 600 °C	500 °C, 600 °C, 700 °C

3.2.3 Product analysis and measurement

The produced TCR[®] bio-oil mainly for viscosity, TAN, and composition were analyzed. A Mettler Toledo T50 was used to determine the TAN following the ASTM D664-04 standard. The viscosity of the oil was measured at 40 °C using the rotational rheometer RheolabQC following the ASTM D5018 method. The composition of the bio-oil was analyzed through gas chromatography-mass spectroscopy (GC-MS). This GC uses 5% a phenyl methyl siloxane capillary column 30 meters in length, 0.25 mm in diameter, and 0.25 in micrometer film thickness. A small amount of bio-oil (10%) is mixed with dichloromethane as solvent (90%). The mixture was analyzed after being micro-centrifuged and filtered with a 2-micron PTFE filter. A testing sample of 1 µL was introduced into the column with the help of helium carrier gas, and the GC-MS operation was done

in splitless mode. The temperature was kept constant at 50 °C for 5 minutes, then ramped by 10 °C/minute to 325 °C and held there for 7.5 minutes. The auxiliary interface between GC and MS was maintained at 280 °C. The compounds in the chromatograph were identified through the NIST library [54] based on corresponding surface area to the total surface area of the identified peaks.

A CP-4900 Micro Gas Chromatograph (GC) was used to quantify the gases produced in the experiments. Each column has a miniature GC with an electronic carrier gas control, micro-machined injector, narrow-bore analytic column, and micro thermal conductivity detector (μ TCD). Helium and argon are used as carrier gases, and the GC can quantify gases such as CO, CO₂, H₂, N₂, O₂, CH₄, and C_xH_y. Though the Micro GC model has four columns, three were used in the analysis. The total yield of the syngas was calculated based on the mass balance difference. The Micro GC was baked out for 22 hours and calibrated through standard gas samples at regular intervals between experiments.

3.3 Results and discussion

3.3.1 Mass and energy balances

The yields of bio-oil, char, syngas, and the aqueous phase produced from the thermo-catalytic reforming of softwood pellets in a lab-scale TCR[®]-2 plant at different experimental conditions are shown in Table 3.3. The yields were calculated by wt. % except the total gas yield, which was calculated by the difference using the following equation:

$$\text{Total gas yield \%} = 100 - \text{bio-oil wt. \%} - \text{aq. phase wt. \%} - \text{biochar yield wt.\%}$$

Table 3.3. Mass balance of the TCR products from processing of softwood pellets

SN	Reactor temperature (°C)	Reactor temperature (°C)	Bio-oil %	Char %	Aq. phase %	Syngas % (a)
1	400	500	7.99	21.46	23.39	47.16
2	400	600	3.42	18.68	15.93	61.97
3	500	600	3.49	15.80	14.76	65.95
4	400	700	1.99	17.12	12.67	68.22
5	450	700	2.22	17.66	14.55	65.57
6	500	700	1.82	15.82	10.21	72.15
7	550	700	2.15	15.71	11.41	70.73
8	600	700	1.69	15.29	10.44	72.58

(a) Calculated by difference.

The mass balance shows that the maximum bio-oil yield was 7.99 wt. % at a reactor temperature of 400 °C and a reformer temperature of 500 °C, and the minimum (1.69 wt. %) yield was reached at a reactor temperature of 600 °C and a reformer temperature of 700 °C. The maximum biochar yield (21.46 wt. %) was reached at a reactor temperature of 400 °C and a reformer temperature of 500 °C and the minimum (15.29 wt. %) at a reactor temperature of 600 °C and a reformer temperature of 700 °C. Syngas follows the opposite trend: the minimum (47.16 wt. %) and maximum (72.58 wt. %) yields were reached at 400 °C/500 °C and 600 °C/700 °C reactor-reformer temperatures, respectively. The aqueous phase follows a similar trend to bio-oil and biochar for the maximum (23.39 wt. %) and minimum (10.21 wt. %) yields. This mass balance calculation has accuracy limitations due to the loss of feedstock and char in the form of dust and liquid products sticking to the walls of the pipes and vessels.

Table 3.4. Energy balance of the TCR products from processing of softwood pellets

Reactor temperature (°C)	Reactor temperature (°C)	% Bio-oil	% Biochar	% Aq. phase	% Syngas	% Conversion	% Losses
400	500	14.35	38.97	0.00	17.45	70.77	29.23
400	600	6.46	33.47	0.00	19.13	59.06	40.94
500	600	6.57	28.35	0.00	16.90	51.82	48.18
400	700	3.81	30.18	0.00	20.33	54.32	45.68
450	700	4.30	32.54	0.00	12.57	49.41	50.59
500	700	3.52	28.32	0.00	15.07	46.91	53.09
550	700	4.17	27.77	0.00	23.41	55.35	44.65
600	700	3.27	27.49	0.00	27.03	57.80	42.20

The energy balances for the whole set of experiments are listed in Table 3.4. The maximum conversion rate of 70.77% was observed at a reactor temperature of 400 °C and a reformer temperature of 500 °C. The minimum conversion rate (46.91%) was observed in the experiment with reactor and reformer temperatures of 500 °C and 700 °C, respectively. The conversion % was calculated by adding the individual energy contents of the valorized products and the loss % was calculated by subtracting the sum of the individual energy contents of the products from the total feedstock energy content.

Reforming temperature is one of the major factors affecting the quality and quantity of valorized TCR products. This study was performed to understand the effect of reforming temperature. For this purpose, the reactor temperature was fixed at 400 °C and the reformer temperature was maintained in the experiments at 500 °C, 600 °C, and 700 °C. The resulting bio-oil, biochar, and syngas were collected and analyzed to understand the effect of reforming temperature on quantity and quality.

3.4 The effect of reformer temperature

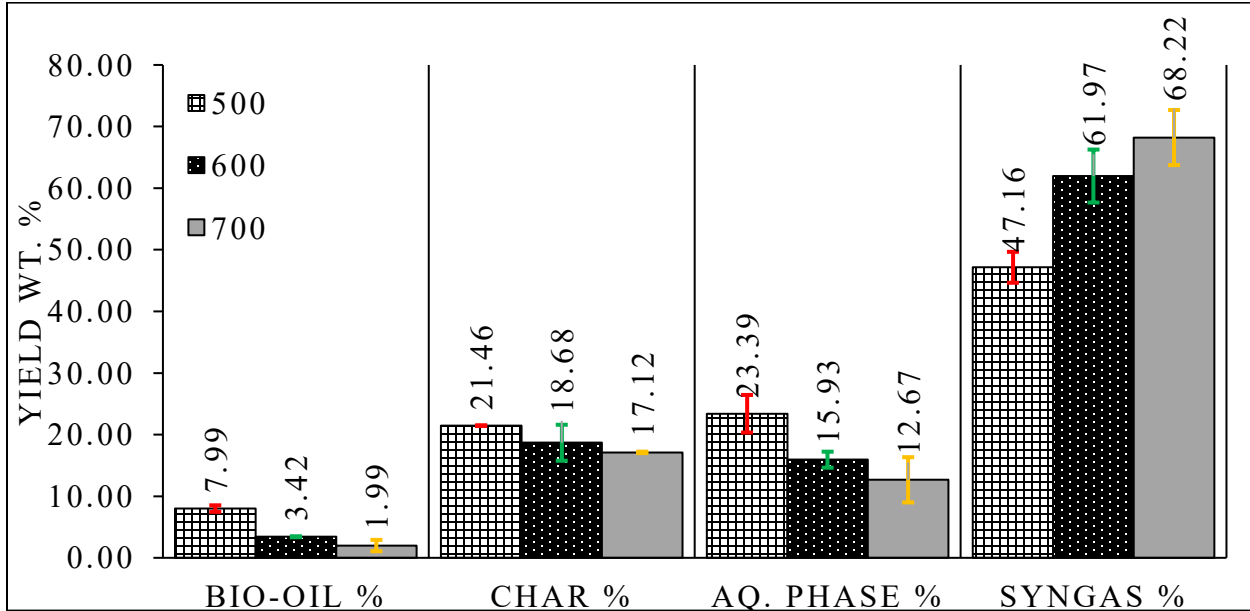


Figure 3.2. Mass balance of TCR products from processing of softwood pellet at different reformer temperatures

Table 3.5. Post-reforming reactions (from Neumann et al. [43])

Reaction	Enthalpy	Number
$\text{CO}_2 + \text{C} \rightleftharpoons 2\text{CO}$	+172	1
$\text{C} + \text{H}_2\text{O} \rightleftharpoons \text{CO} + \text{H}_2$	+131	2
$\text{C} + 1/2\text{O}_2 \rightleftharpoons \text{CO}$	-111	3
$\text{CH}_4 + \text{H}_2\text{O} \rightleftharpoons 2\text{CO}$	+206	4
$\text{CO} + \text{H}_2\text{O} \rightleftharpoons \text{CO}_2 + \text{H}_2$	-41.2	5
$\text{C} + \text{H}_2 \rightleftharpoons \text{CH}_4$	-74.8	6

Figure 3.2 shows the effect of reforming reactions on the product distribution of bio-oil, syngas, char, and the aqueous phase. Bio-oil, char, and aqueous phase yields decrease with an increase in reforming temperature, and syngas yield shows the opposite trend. Char yields were 21.46 wt. %, and syngas yield was 47.16 wt. % at 500°C.

18.68 wt. %, and 17.20 wt. % with reformer temperatures of 500 °C, 600 °C, and 700 °C, respectively. Bio-oil yield decreased significantly with an increase in reforming temperature. The maximum yield (7.994 wt. %) was obtained at a reforming temperature of 500 °C and the minimum (1.995 wt. %) at a reforming temperature of 700 °C. Syngas yield increased significantly (from 47.158 wt. % at 500 °C to 71.379 wt. % at 700 °C). This large increase is mainly due to the reactions shown in Table 3.5, from Neumann et al.'s study on anaerobic digested feedstock [43]. The conversion of char and the cracking of organic vapors into permanent gases, as well as the forward gas shift reaction in the aqueous phase, significantly increased syngas quantity at higher reforming temperatures. These results are comparable with studies by Neumann et al. [43] and Ahmad et al. [25] on anaerobic digestate and RSB (residual sugarcane bagasse), respectively.

3.4.1 Biochar characterization

Table 3.6. CHNS analysis of softwood pellet-based biochar for a fixed reactor temperature and different reformer temperatures

Reformer temperature (°C)	Ultimate analysis (dry basis) (wt. %)		
	500	600	700
Carbon	89.77	90.18	93.60
Hydrogen	2.23	1.68	0.84
Nitrogen	0.18	0.17	0.15
Sulfur	0.00	0.00	0.00
Oxygen(a)	7.83	7.97	5.41
O/C	0.087	0.088	0.058
H/C	0.025	0.019	0.009
HHV (MJ/kg)	35.06	34.59	34.53

Table 3.6 shows the CHNS analysis of the char produced at different reforming temperatures. Hydrogen and nitrogen decrease with an increase in reforming temperature, whereas carbon content increases with an increase in reforming temperature. Carbon content was lowest (89.77

wt. %) at 500 °C and highest (93.60 wt. %) at 700 °C. There was minimal effect on the HHV of the char; it was found to be 35.06, 34.59, and 34.53 MJ/kg at 500 °C, 600 °C, and 700 °C, respectively. However, Jäger et al. reported the highest HHV at 600 °C in the range of 25 to 30 MJ/kg [45]. Overall O/C and H/C ratios show a decreasing trend, which indicates char's higher stability during reforming reactions. Jäger et al. argued that for char to be used as soil conditioner and for long term carbon sequestration, char with a lower O/C is preferred, and an O/C ratio below 0.05 indicates the superior quality of biochar produced [45].

3.4.2 Bio-oil characterization

Table 3.7 shows the properties of the bio-oil produced at three reformer temperatures (400 °C, 500 °C, and 600 °C) at a fixed reactor temperature of 400 °C. The total oxygen content decreases sharply with an increase in reforming temperature. The highest wt. % of oxygen (25.56 wt. %) was found in bio-oil at a reforming temperature of 500 °C and the lowest (12.88 wt. %) at a reforming temperature of 700 °C. The total reduction of oxygen content was justified by reforming reactions of oxygenated compounds forming permanent gases at higher reformer temperatures. Ahmad et al. performed an experiment on sugarcane bagasse at three reforming temperatures (500, 600 and 700 °C) at a fixed reactor temperature of 500 °C [25]. The highest bio-oil oxygen content (35.2 wt. %) was observed at 500 °C and the lowest (10.2 wt. %) at a 700 °C reformer temperature. The results presented in Table 3.7 follow this trend. TAN and viscosity show a similar trend: they decrease with an increase in reformer temperature. The TAN ranges from a maximum of 22.233 mg KOH/g to a minimum of 7.959 mg KOH/g and viscosity ranges from a maximum of 43.1 mPas to a minimum of 20.6 mPas. The results for the TAN show the opposite trend as Ahmad et al.'s results for sugarcane bagasse [25] and may be due to differences in feedstock type and reactor temperature. The total hydrogen content decreased with an increase in reformer temperature and

was found to be 7.027, 6.629, and 6.190 wt. % at reforming temperatures of 500 °C, 600 °C, and 700 °C, respectively. The O/C and H/C ratios decrease with an increase in reforming temperature, which shows the improvement in bio-oil quality with increased reformer temperature. The total O/C ratio was reduced by almost 58% from 0.38 at a 500 °C reforming temperature to 0.16 at a 700 °C reformer temperature. Similarly, the H/C ratio decreased by nearly 27% to 0.105 at a 500 °C reforming temperature and 0.077 at 700 °C. The O/C and H/C results were validated against the results published by Ahmad et al. for sugarcane bagasse [25].

Table 3.7. Softwood pellet-based bio-oil properties at a fixed reactor temperature of 400 °C

Reformer temperature (°C)	Ultimate analysis (dry basis) (wt. %)		
	500	600	700
Carbon	67.203	76.517	80.326
Hydrogen	7.027	6.629	6.190
Nitrogen	0.206	0.342	0.610
Sulfur	0.000	0.000	0.000
Oxygen	25.564	16.512	12.875
O/C	0.380	0.216	0.160
H/C	0.105	0.087	0.077
TAN (mg KOH/g)	22.233	21.205	7.959
Viscosity (mPas)	43.1	36.9	20.6
HHV (MJ/kg)	34.672	36.491	36.935

Table 3.8. GC-MS analysis of softwood pellet-based bio-oil at a fixed reactor temperature and different reformer temperatures

% Area (Compound type)	Reformer temperature (°C)		
	500	600	700
MAHs	-	11.2	10.7
PAHs	-	16.0	43.1
FAMEs	-	-	5.8
N-compound	-	-	0.6
O-compound	5.9	7.8	8.9
Phenol & alcohol	94.1	53.8	18.3
Acids	-	-	-
Total detection	100.0	88.9	87.5

Table 3.8 shows the seven types of compounds found in bio-oil from three experiments at different reformer temperatures, and Table 3.9 shows the entire list of compounds detected by the GC-MS. Bio-oil is a mixture of compounds; for ease of the analysis of bio-oil composition, any compound that occupies less than 3% of the largest peak is neglected in the study. The PAHs and O-compounds increase with an increase in reformer temperature, and phenol and alcohol levels decrease. At higher reforming temperatures, phenol and alcohol undergo secondary cracking reactions such as deoxygenation and yield more aromatic, as noted by Ahmad et al. [25]. Bio-oil produced at a reformer temperature of 500 °C mainly contains phenol and its derivatives (i.e., phenol, 3-methyl-; 1,2-benzenediol, 4-methyl-; phenol, 2,4-dimethyl-; phenol, 2-methyl-; creosol, catechol, phenol at 18.18%, 12.98%, 8.58%, 8.05%, 7.38%, 6.10%, and 6.0%, respectively). Similarly, for a reformer temperature of 600 °C, the amount of phenol and its derivatives reduced significantly to 53.8%; at this temperature, 11.2% MAHs and 16% PAHs were observed. Some fraction of O-compounds like benzofuran and its derivatives also appear at this temperature. At a reformer temperature of 700 °C, there was a significant increase in PAHs and FAMES (fatty acid methyl esters), while the amount of MAHs was similar to that at the reformer temperature of 600 °C. The HHV of bio-oil produced at a 600 °C reformer temperature, 36.5 MJ/kg, was similar to the range (33.6 to 35.5 MJ/kg) found by Jäger et al. for woody feedstock [45].

Table 3.9. Total compound GC-MS analysis of softwood pellet-based bio-oil at a fixed reactor temperature and different reforming temperatures

SN	Compound name	Reformer temperature (°C)		
		500	600	700
1	Bicyclo -4.2.0- octa-1,3,5-triene	-	2.00	-
2	Benzofuran	-	1.85	1.79
3	Phenol	6.00	13.47	6.53
4	Indene	-	4.11	6.62
5	Acetic acid, phenyl ester	-	-	4.10

SN	Compound name	Reformer temperature (°C)		
		500	600	700
6	Phenol, 2-methyl-	8.05	8.06	2.96
7	p-Cresol	-	19.16	5.76
8	Benzofuran, 2-methyl-	-	1.55	0.48
9	Benzene, 1-butynyl	-	1.47	-
10	Phenol, 2,4-dimethyl-	8.58	6.16	-
11	Acetic acid, 4-methylphenyl ester	-	-	1.69
12	Naphthalene	-	4.54	18.86
13	Naphthalene, 2-methyl-	-	-	5.05
14	Biphenyl	-	-	1.07
15	Naphthalene, 2-ethenyl-	-	-	1.62
16	Biphenylene	-	2.82	6.03
17	1,1'-Biphenyl, 4-methyl-	-	-	0.24
18	Dibenzofuran	-	-	1.08
19	Naphthalene, 2-(1-methylethenyl)-	-	-	0.52
20	Fluorene	-	1.04	1.92
21	Phenanthrene	-	1.56	0.64
22	Phenanthrene, 1-methyl-	-	-	0.51
23	4H-Cyclopentaphenanthrene	-	-	0.87
24	Tricyclo8.2.2.2(4,7) hexadeca-2,4,6,8,10,12,13,15-octaene	-	-	0.47
25	Fluoranthene	-	-	0.63
26	Isothiazol-5-amine, 4-bromo-3-chloro-N-methyl-	-	-	0.39
27	Benzene, 1-ethenyl-3-methyl-	-	1.38	1.09
28	1H-Indene, 1-methyl-	-	2.28	1.09
29	Phenol, 4-ethyl-	-	1.05	-
30	Phenol, 3-ethyl-	5.27	2.90	0.61
31	Benzofuran, 2,3-dihydro-	-	2.53	0.77
32	Phenol, 3-(1-methylethyl)-	-	2.33	-
33	Cyclohexasiloxane, dodecamethyl-	-	1.88	-
34	Naphthalene, 1-methyl-	-	2.60	3.33
35	7-Chloro-2,3-dihydro-3-(4-N, N-dimethylaminobenzylidene)-5-phenyl-1H-1,4-benzodiazepin-2-one	-	1.82	-
36	1H-Indenol	4.04	0.67	-
37	Naphthalene, 2,6-dimethyl-	-	1.64	-
38	Phenol, 3,5-dimethyl-	-	-	1.37
39	1,2-Benzenediol, 4-methyl-	12.98	-	-
40	Benzofuran, 7-methyl-	-	-	1.38
41	2-Naphthalenol	-	-	0.09
42	Phenol, 3-methyl-	18.18	-	-

SN	Compound name	Reformer temperature (°C)		
		500	600	700
43	Catechol	6.10	-	-
44	Creosol	7.38	-	-
45	Phenol, 4-ethyl-2-methoxy-	4.24	-	-
46	1,2-Benzenediol, 3-methyl-	4.11	-	-
47	2-Methoxy-4-vinylphenol	4.98	-	-
48	Benzene, 1,4-dimethoxy-	5.87	-	-
49	Phenol, 2-methoxy-4-(1-propenyl)-	4.22	-	-
50	Styrene	-	-	1.89
51	Benzene, (2-propenyloxy)-	-	-	0.42
52	Benzene, 1,1'-(diazomethylene)bis-	-	-	0.63
53	1-Naphthalenol	-	-	0.60
54	m-Cresyl acetate	-	-	0.51
55	1H-Phenalene	-	-	0.53
56	2-Propenal, 3-phenyl-	-	-	0.76
57	Benzene, butoxy-	-	-	0.70
58	Naphthalene, 1,7-dimethyl-	-	-	0.49
59	2-Naphthyl carbamate	-	-	0.53
60	Dibenzofuran, 4-methyl-	-	-	0.52
61	1H-Indene, 2-phenyl-	-	-	0.36
Total % of gas detection		100.00	88.86	87.51

3.4.3 Permanent gas composition and properties of softwood pellets

Table 3.10. Micro GC gas composition with a fixed reactor temperature and different reformer temperatures

Reformer temperature (°C)	Gas composition vol. %		
	500	600	700
C ₃ +	0.74	0.37	0.67
Hydrogen	10.46	14.46	24.21
Methane	31.41	29.80	26.37
Carbon monoxide	18.42	22.77	37.79
Carbon dioxide	37.92	31.61	10.13
C ₂	0.72	0.48	0.56
H ₂ S	0.00	0.00	0.00
C ₃	0.32	0.52	0.27
HHV (MJ/kg)	13.40	14.68	20.85
LHV(MJ/kg)	8.16	8.47	9.31

Table 3.10 shows the composition of gas detected by the Micro GC for three experiments. The amount (vol. %) of C₂, C₃, and C₃₊ remains almost constant at all reforming temperatures. The main results from Table 10 are summarized in Figure 3.3. The main gas yields in processing of softwood pellets at a fixed reactor temperature and different reformer temperatures. With an increase in reforming temperature, the amounts of hydrogen and carbon monoxide increase. Hydrogen concentration increased by 132% from 10.46 vol. % at a 500 °C reformer temperature to 24.21 vol. % at 700 °C. This increase in the hydrogen concentration is mainly due to the reforming reactions of bio-oil vapors on the surface of biochar [25]. Similarly, the carbon monoxide yield increased by 100% and reached 37.79 vol. % at 700 °C compared to 500 °C. The highest methane yield (31.41 vol. %) was observed at 500 °C and the lowest (26.37 vol. %) at 700 °C. The carbon dioxide amount decreased with an increase in reforming temperature by almost 75% and reached 10.13 vol. % at 700 °C. The HHV of syngas produced at 400 °C (reactor) and 600 °C (reformer) is 14.68 MJ/kg, which is comparable to the results (14.6 to 14.9 MJ/kg) by Jäger et al. for woody biomass [45].

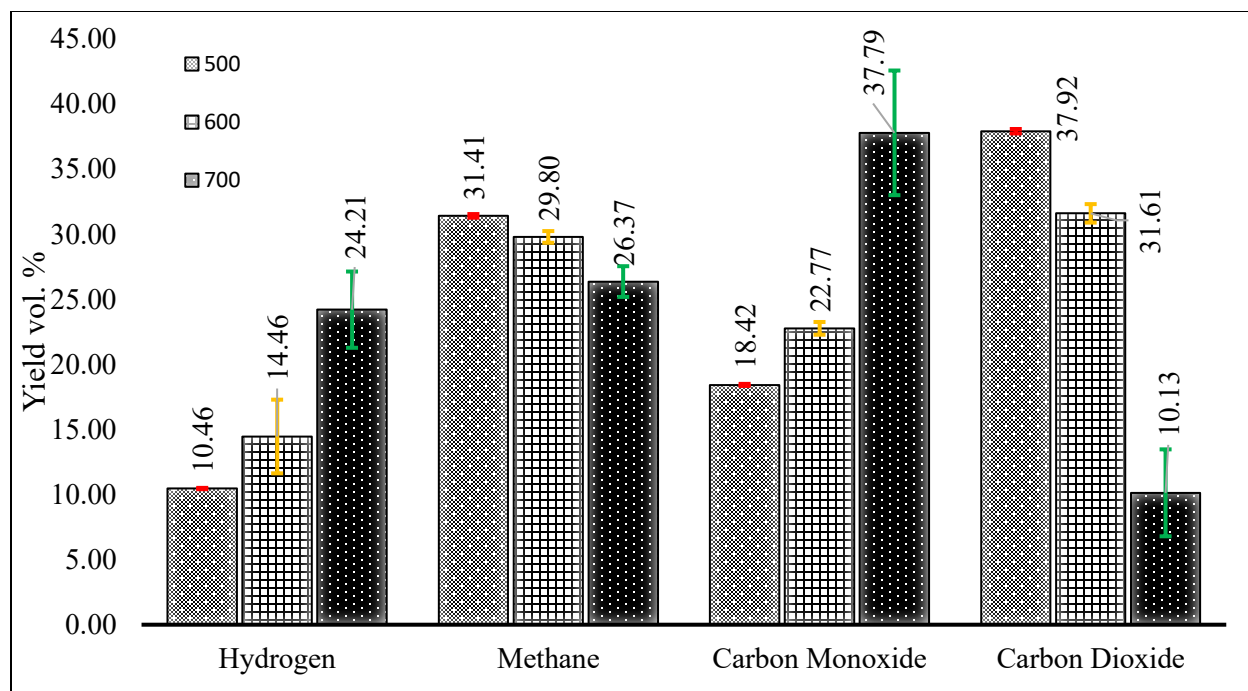


Figure 3.3. The main gas yields in processing of softwood pellets at a fixed reactor temperature and different reformer temperatures through a TCR unit

3.5 The effect of reactor temperature

For this set of experiments, the reformer temperature was fixed at 700 °C and the reactor temperature was changed from 400 to 600 °C. Figure 3.4 shows the distribution of the valorized products. The total bio-oil, biochar, aqueous phase, and syngas yields were similar. There is a slight increase in the syngas yield with an increase in reactor temperature, from 68.22 wt. % at 400 °C to 72.58 wt. % at 600 °C. However, bio-oil yield decreased from 1.99 wt. % at 400 °C to 1.69 wt. % at 600 °C. The post-reforming temperature of 700 °C increased the permanent gas yield because of reactions 1, 2, 3, and 6 (shown in Table 5). The post-reforming process was facilitated by reaction 5, the water gas shift reaction.

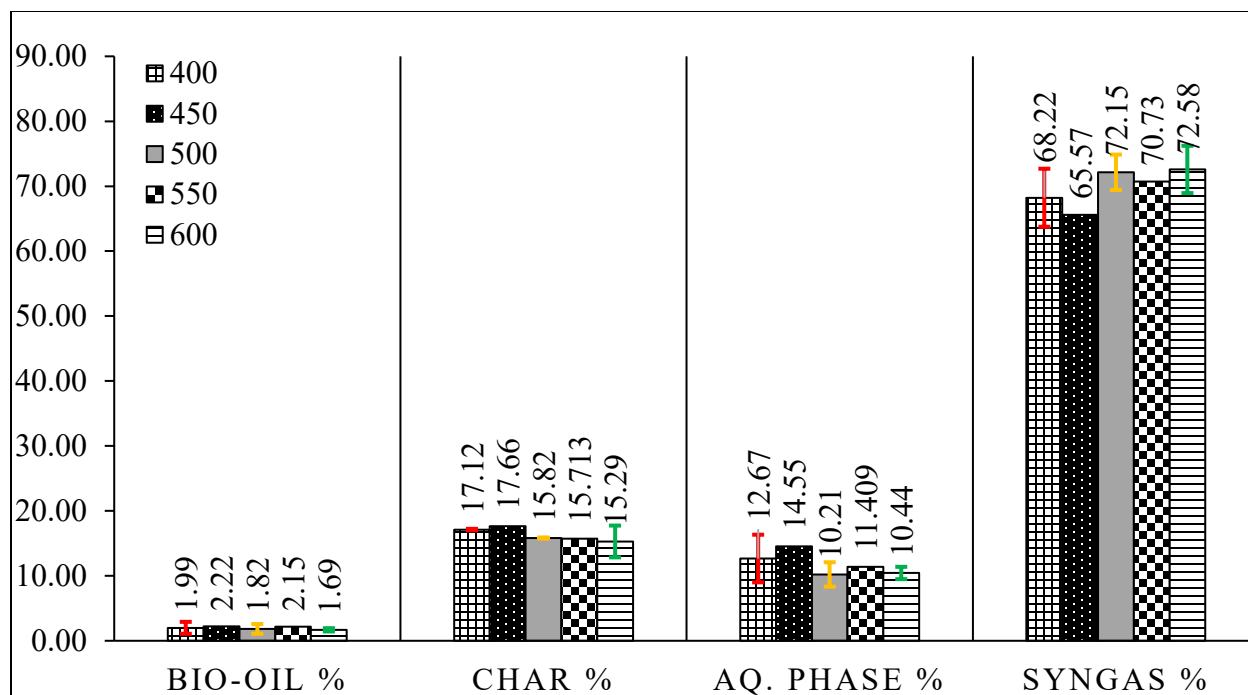


Figure 3.4. Mass balance at different reactor temperatures for processing of softwood pellets in a TCR unit

3.5.1 Biochar characterization

Table 3.11 shows the proximate analysis of the softwood pellet-based biochar produced at different reactor temperatures. The maximum HHV of char (34.71 MJ/kg) was found at 600 °C and the minimum (34.53 MJ/kg) at 400 °C. The maximum O/C ratio (0.060) was at 550 °C, which shows the stability of biochar, and the minimum (0.054) at 450 and 600 °C. Overall, the H/C ratio remains almost constant at all reactor temperatures. The higher heating value of biochar produced remains almost constant at 34.5 MJ/kg. A similar study by Neumann et al. using digestate as feedstock at a reformer temperature of 750 °C and reactor temperature of 400 °C produced biochar with an HHV of 33.9 MJ/kg [71].

Table 3.11. CHNS analysis of softwood pellet-based biochar at a fixed reforming temperature and different reactor temperatures

	Ultimate analysis, dry basis (wt. %)				
	Reactor temperature (°C)				
	400	450	500	550	600
Carbon	93.60	93.54	93.80	92.03	93.82
Hydrogen	0.84	1.23	0.83	0.88	0.96
Nitrogen	0.15	0.12	0.16	1.61	0.15
Sulphur	0.00	0	0.00	0.00	0.00
Oxygen (a)	5.41	5.11	5.21	5.48	5.07
O/C	0.058	0.054	0.056	0.060	0.054
H/C	0.009	0.01	0.009	0.010	0.010
HHV (MJ/kg)	34.53	32.37	34.57	34.12	34.71

3.5.2 Softwood pellet-based bio-oil characterization

The proximate analysis results of the bio-oil formed at different reactor temperatures and a fixed reformer temperature of 700 °C are shown in Table 3.11. The total carbon (wt. %) increases with an increase in reactor temperature. However, the hydrogen and oxygen contents show the opposite trend. The HHV of bio-oil (37.475 MJ/kg) was highest at 700 °C and the lowest (34.25 MJ/kg) at 450 °C. The overall decrease in O/C and H/C ratios shows the stability of bio-oil. The viscosity of bio-oil reduced with an increase in reformer temperature to 50.9, 28.4, 18.30, and 11.9 mPas at reactor temperatures of 400, 500, 500, and 600 °C, respectively. The TAN similarly decreases with an increase in reactor temperature. The viscosity was 14.411 mg KOH/g at a 400 °C reactor temperature, 8.120 mg KOH/g at 500 °C, and 3.140 mg KOH/g at 600 °C. Similar experiments were performed by Conti et al. on bark-free beech wood chips at 400 °C reactor and 700 °C reformer temperatures and their results showed a TAN of 5.4 mg KOH⁻¹ and an HHV of the bio-oil produced of 35.3 MJ/kg with oxygen content up to 17% [48]. The results of the present study produced bio-oil of good quality. Neumann et al. reported a TAN of 5.1 mg KOH⁻¹ and viscosity

of 40 mm²/s for bio-oil produced from anaerobic digestate at 450 °C reactor and 750 °C reformer temperatures [43].

Comprehensive analysis results of the GC-MS of bio-oil are shown in Table 3.13; the results were divided into seven categories and plotted (Figure 3.5). There was a significant drop in the O-compound in the bio-oil with an increase in the reactor temperature. The highest MAH yield (13.7%) was at a reactor temperature of 450 °C and the lowest (11.6) at a 400 °C reactor temperature. PAHs increase with an increase in reactor temperature; at a 600 °C reactor temperature, more than half (52.4%) of the bio-oil is made up of PAHs. Phenol and alcohol, however, decrease with an increase in reactor temperature as at higher temperatures, they are reduced to more permanent gases.

Table 3.12. Proximate analysis results of softwood pellet-based bio-oil prepared at a fixed reforming temperature and different reactor temperatures

	Ultimate analysis (dry basis) (wt. %)				
	Reactor temperature (°C)				
	400	450	500	550	600
Carbon	80.326	80.44	81.956	82.254	82.539
Hydrogen	6.190	6.66	6.171	6.224	6.199
Nitrogen	0.610	0.35	0.625	0.522	0.672
Sulfur	0.000	0	0.000	0.000	0.000
Oxygen	12.875	11.78	11.248	10.980	10.590
O/C	0.160	0.1464	0.137	0.133	0.128
H/C	0.077	0.0827	0.075	0.076	0.075
TAN (mg KOH/g)	14.411	6.53±1.15	8.120	6.1995	3.140
Viscosity (mPas)	50.900	13.77	28.400	18.300	11.900
HHV (MJ/kg)	36.935	34.25	37.307	37.46	37.475

Table 3.13 Complete set of compounds detected by the GC-MS at a fixed reformer temperature and different reactor temperatures in processing of softwood pellet in a TCR unit

SN	Compound name	Reactor temperature				
		400	450	500	550	600
		%	%	%	%	%
1	(Z)-1-Phenylpropene	-		1.25	1.268	-

SN	Compound name	Reactor temperature				
		400	450	500	550	600
		%	%	%	%	%
2	1,1'-Biphenyl, 3-methyl-		0.82			
3	1,3-Benzenediol, 4-propyl-		1.44			
4	1H-Benzo(a)fluorene		0.26			
5	1H-Imidazo(4,5-d)pyridazine		14.43			
6	1H-Phenalene		4.24		0.6209	
7	1-Naphthalenol	-	0.38	0.38	0.5238	0.61
8	2-Methylindene	-		0.63		-
9	2-Naphthalenol		1.28			
10	2-Propenoic acid, 3-(2-naphthalenyl)-		0.37			
11	3H-Benz(e)indene, 2-methyl-		0.24			
12	3-Hydroxyphenylacetylene	-		-	1.7891	1.72
13	4H-Cyclopenta phenanthrene	-		0.58	0.7242	0.53
14	5-Acetyl-2-methylpyridine	-		-		1.37
15	9,10-Bis(bromomethyl)anthracene		1.56			
16	9H-Fluoren-9-one		0.33			
17	9H-Fluorene, 1-methyl-		0.45			
18	9H-Fluorene, 9-methyl-	-		0.63		-
19	Acenaphthene		0.34			
20	Acetic acid, 4-methylphenyl ester	1.05	7.36	1.05		2.54
21	Acetic acid, phenyl ester	1.97		2.55	3.033	3.77
22	Anthracene		1.48			
23	Anthracene, 1,2-dihydro-	-		-		0.7
24	Anthracene, 9-methyl-		1.59			
25	Benzaldehyde, 2-methyl-	-		0.39		-
26	Benzaldehyde, 3,5-dichloro-2-hydroxy-		0.31			
27	Benzaldehyde, 3-methyl-	1.59	1.07	-		-
28	Benzene, (2-propenyloxy)-	-		0.38		-
29	Benzene, 1,1'-(1,3-butadiyne-1,4-diyl) bis-	-		0.46		-
30	Benzene, 1,1'-(diazomethylene)bis-	-		0.5	0.7197	0.56
31	Benzene, 1-butynyl	-		1.13		0.87
32	Benzene, 1-butynyl		1.53		0.4688	
33	Benzene, 1-ethenyl-3-methyl-	1.38		-		-
34	Benzene, 1-propynyl-	7.52		7.69		-
35	Benzene, 2-propenyl	-		-		1.03
36	Benzene,2,6-dimethyl-1(phenylmethyl)-		0.27			
37	Benzeneethanamine, N-(3-chloropropyl)-. alpha.-methyl-	1		-		-

SN	Compound name	Reactor temperature				
		400	450	500	550	600
		%	%	%	%	%
38	Benzo(b)benzofuran-2-carboxaldehyde		7.11			
39	Benzofuran	1.92		1.89		-
40	Benzofuran, 2,3-dihydro-	1.76	0.35	1.06	0.533	-
41	Benzofuran, 2-methyl-	-		1.09		-
42	Benzofuran, 4,7-dimethyl-		0.86			
43	Benzofuran, 7-methyl-	1.18		0.67	1.0874	1.04
44	Bicyclo(4.2.0)octa-1,3,5-triene		2.4		2.0454	
45	Biphenyl	-		1.04	1.1784	1.2
46	Biphenylene	5.81		5.95	7.0037	7.59
47	Dibenzofuran	1.38		1.09	1.1611	1.29
48	Dibenzofuran, 4-methyl-		0.49			
49	Dibenzofuran, 4-methyl-		1.01			
50	Fluoranthene	1	1.33	0.58	0.7541	0.8
51	Fluorene	1.7		0.59	2.0504	2.22
52	Fluorene		0.61			
53	Indene	-	3.88	-	8.1239	8.24
54	Isothiazol-5-amine, 4-bromo-3-chloro-N-methyl-	-		0.46	0.5561	-
55	m-Cresyl acetate		0.92		1.18	
56	Naphthalene	18.43	0.33	21.13	20.692	24.62
57	Naphthalene, 1,2-dihydro-	1.42		-		-
58	Naphthalene, 1,2-dihydro-		0.83		1.1343	
59	Naphthalene, 1,4-dimethyl-		7.31			
60	Naphthalene, 1,6-dimethyl-		0.68			
61	Naphthalene, 1-methyl-	-		5.04	5.5247	5.99
62	Naphthalene, 2-(1-methylethenyl)-	-	0.65	-	0.6417	0.54
63	Naphthalene, 2,7-dimethyl-	-	1.7	0.46	0.6357	0.53
64	Naphthalene, 2-ethenyl-	1.24		1.71	2.0701	1.66
65	Naphthalene, 2-methyl-	5.03	2.08	3.19		-
66	p-Cresol	-		7.37	5.9558	-
67	Phenanthrene	3.41	1.66	2.97	0.5995	4.41
68	Phenanthrene, 1-methyl-	-	0.43	-		0.51
69	Phenanthrene, 2-methyl-		0.52		0.5413	
70	Phenol	10.08	8.76	8.23	7.3063	5.59
71	Phenol, 2,4-dimethyl-	2.53	0.95	1.78	1.4188	1.08
72	Phenol, 2-methyl-	4.49	11.62	3.92	3.3127	2.4
73	Phenol, 3,4-dimethyl-	1.53		0.83		-
74	Phenol, 3,5-dimethyl-	2.78		-		-

SN	Compound name	Reactor temperature				
		400	450	500	550	600
		%	%	%	%	%
75	Phenol, 3-methyl-	9.99	1.52	-		4.42
76	Phenol, 4-ethenyl-, acetate	-		0.55		0.57
77	Phenol, 4-ethyl-		0.29			
78	Phenol, 4-ethyl-2-methoxy-		0.38			
79	Pyrene	-	0.67	-		1.12
80	Pyrene, 1-methyl-		0.34			
81	Styrene	2.75		2.48		2.11
82	Triphenylene					
	Total Detection	92.94	99.45	91.67	84.65	91.63

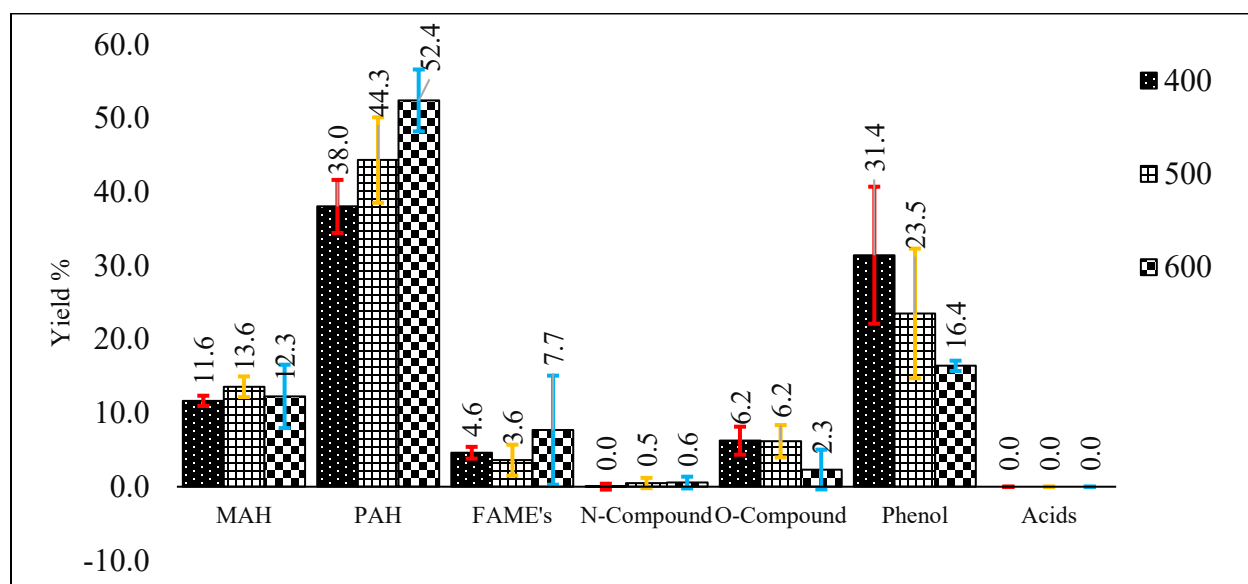


Figure 3.5. Set of compounds from the GC-MS analysis of softwood pellet-based bio-oil at a fixed reforming temperature and different reactor temperatures

3.5.3 Permanent gas composition and properties

Table 3.14. Permanent gas detected by the Micro GC at a fixed reformer temperature and different reactor temperatures in processing of softwood pellets in a TCR unit

Gases	Gas composition (vol. %)				
	Reactor temperature				
	400	450	500	550	600
C ₃ +	0.51	0.37	0.59	0.18	1.01
Hydrogen	20.11	15.09	25.18	12.84	23.74
Methane	27.16	28.28	28.31	22.02	33.93
Carbon monoxide	24.36	24.81	21.21	20.28	19.63
Carbon dioxide	27.45	30.60	24.10	15.34	20.85
C ₂	0.25	0.45	0.38	0.18	0.69
H ₂ S	0.00	0.00	0.00	0.00	0.00
C ₃	0.16	0.39	0.24	0.10	0.15
HHV (MJ/kg)	15.61	14.504	19.48	17.941	20.74
LHV(MJ/kg)	8.56	8.430	9.18	9.175	9.34

The composition of the permanent gas produced from the set of experiments with a fixed reformer temperature is shown in Table 3.14 and Figure 3.6. With an increase in reactor temperature, hydrogen and methane yields increase, whereas carbon dioxide and carbon monoxide yields decrease. C₂, C₃, and C₃+ contents remain almost constant with an increase in the reactor temperature. The HHV of the syngas also increases with an increase in reactor temperature [25]. The highest HHV (20.74 MJ/kg) was observed at a reactor temperature of 600 °C and the lowest (14.504 MJ/kg) at a reactor temperature of 450 °C. These results are comparable with the results published by Ahmad et al. for sugar cane bagasse in a laboratory-scale reactor at a reforming temperature of 700 °C, where the HHV of the syngas produced was 16.17 MJ/kg [25].

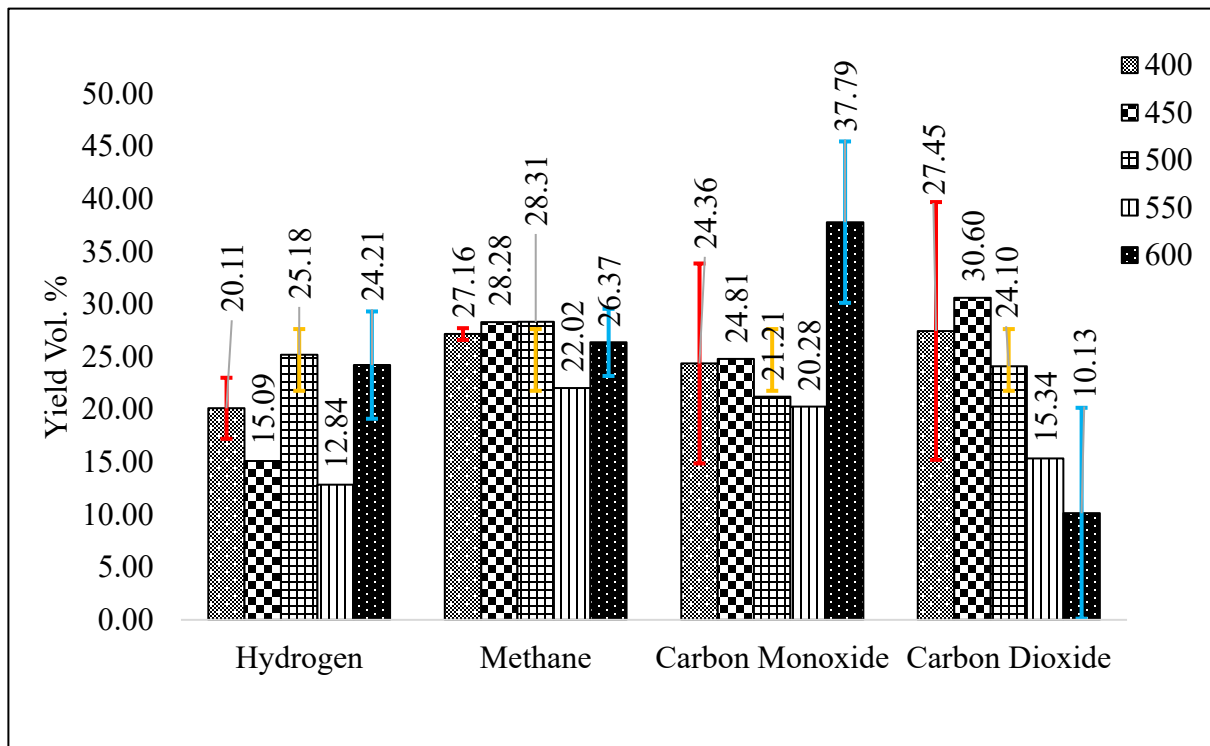


Figure 3.6. The main permanent gas compositions for a fixed reformer temperature (700 °C) and different reactor temperatures in processing of softwood pellets in a TCR unit

3.6 Conclusion

A parametric study was conducted by producing pyrolysis products at different reformer and reactor temperatures. The maximum bio-oil yield (7.994 wt. %) was found at a reactor temperature of 400 °C and a reformer temperature of 500 °C and the minimum (1.69 wt. %) at a 600-700 °C combination of reactor-reformer temperatures. The bio-oil produced is superior to other pyrolysis oils with O/C and H/C ratios of 0.128 and 0.075, respectively. The TAN was found to be as low as 3.14 mg KOH/g and the viscosity as low as 11.9 mPas at 600-700 °C reactor-reformer temperatures. At a higher reformer temperature (700 °C), syngas yield was more than 68 wt. %, irrespective of reactor temperature, and reached a maximum yield (72.58 wt. %) at 600-700 °C (reactor-reformer temperatures). In contrast, the highest char yield (21.46 wt. %) was reached at lower reactor and reformer temperatures of 400 and 500 °C, respectively. It was also observed that

char produced from the experiment was of superior quality as it has a high carbon content (93.82%) and low O/C and H/C ratios. The highest HHV values for bio-oil (37.475 MJ/kg), biochar (35.06 MJ/kg), and syngas (20.854 MJ/kg) were obtained at 600-700 °C, 400-500 °C, and 400-700 °C reactor-reformer temperatures, respectively. Low TAN and viscosity with excellent proportion of PAHs in bio-oil showed the excellent quality of the bio-oil produced. This oil can be mixed with fossil fuel with very less post-treatment. Higher heating value of biochar showed it can be used as a fuel source for various heating processes, furthermore it can be used for soil amendment purpose as well. High heating value of syngas can be utilized for various heating applications, and it can be a source of hydrogen as well.

Chapter 4: Summary, conclusions, and recommendations for future work

4.1 Summary

Thermo-catalytic reforming of Canadian forest and agricultural residues was conducted in a 2 kg/h TCR[®] unit, and a comprehensive analysis of its products such as bio-oil, biochar, and syngas were performed in this study. The TCR[®] product distributions from softwood pellets and wheat straw pellets at a fixed reactor temperature of 400 °C and reformer temperatures of 500, 600, and 700 °C were compared, and the results are shown in Figure 4.1. Wheat straw pellets yield slightly more bio-oil than softwood pellets at all reformer temperatures. But syngas yield was found to be comparatively higher from softwood pellets. At a 700 °C reformer temperature, wheat pellets yield 55.02 wt.% of syngas, whereas at the same temperature, softwood pellets yield almost 68.22 wt.% of syngas. At all reforming temperatures in this study, wheat straw pellets yield more biochar than softwood pellets do. The lowest biochar yield (17.12 wt.%) was observed for softwood pellets at a 700 °C reformer temperature, whereas the highest yield (30.16 wt.%) was observed for wheat straw pellets at 500 °C.

At a high fixed reforming temperature (700 °C), the total bio-oil yield was less than 2.22 wt.%, as shown in Figure 4.2, irrespective of the feedstock type and the reactor temperature. The total char yield from wheat straw pellets was almost 10 wt.% more than that of softwood pellets at all reactor temperatures. At a 550 °C reactor temperature, softwood pellets yield 72.15 wt. % of syngas (the highest), whereas at the same temperature, wheat straw pellets yield 53.18 wt.% of syngas. The total aqueous phase from wheat straw pellets was more than from softwood pellets at every reactor temperature studied.

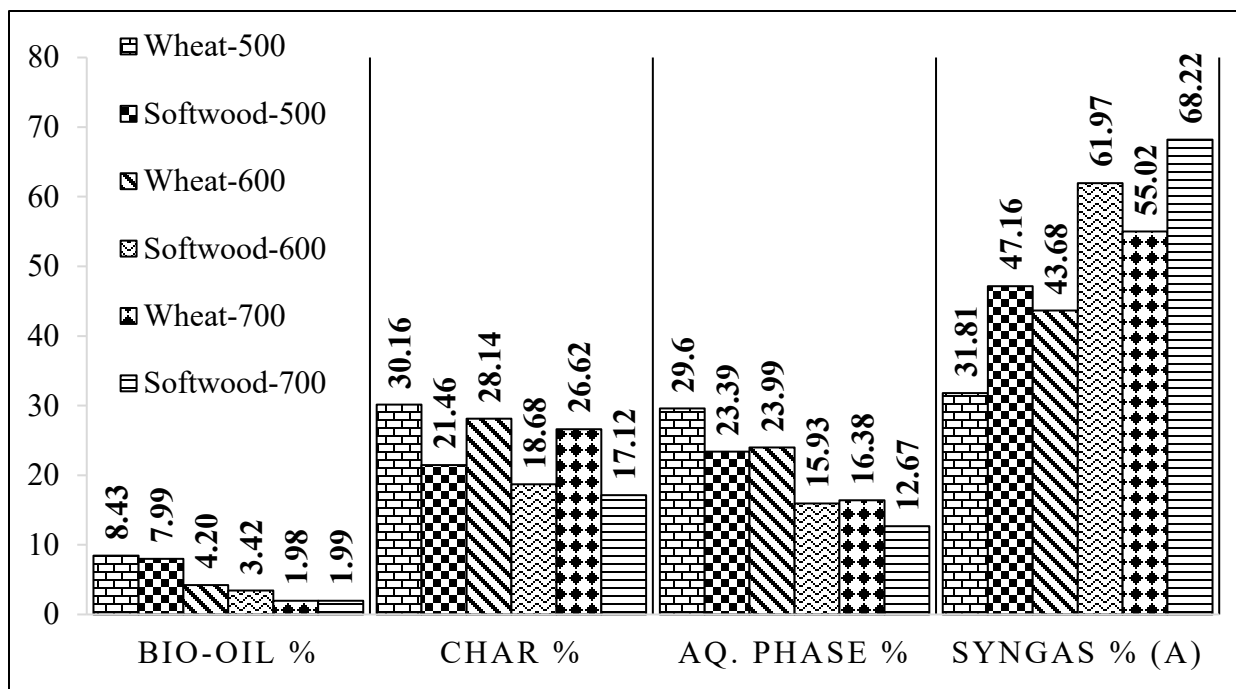


Figure 4.1 TCR product yields from softwood and wheat straw pellets at a fixed reactor temperature of 400 °C

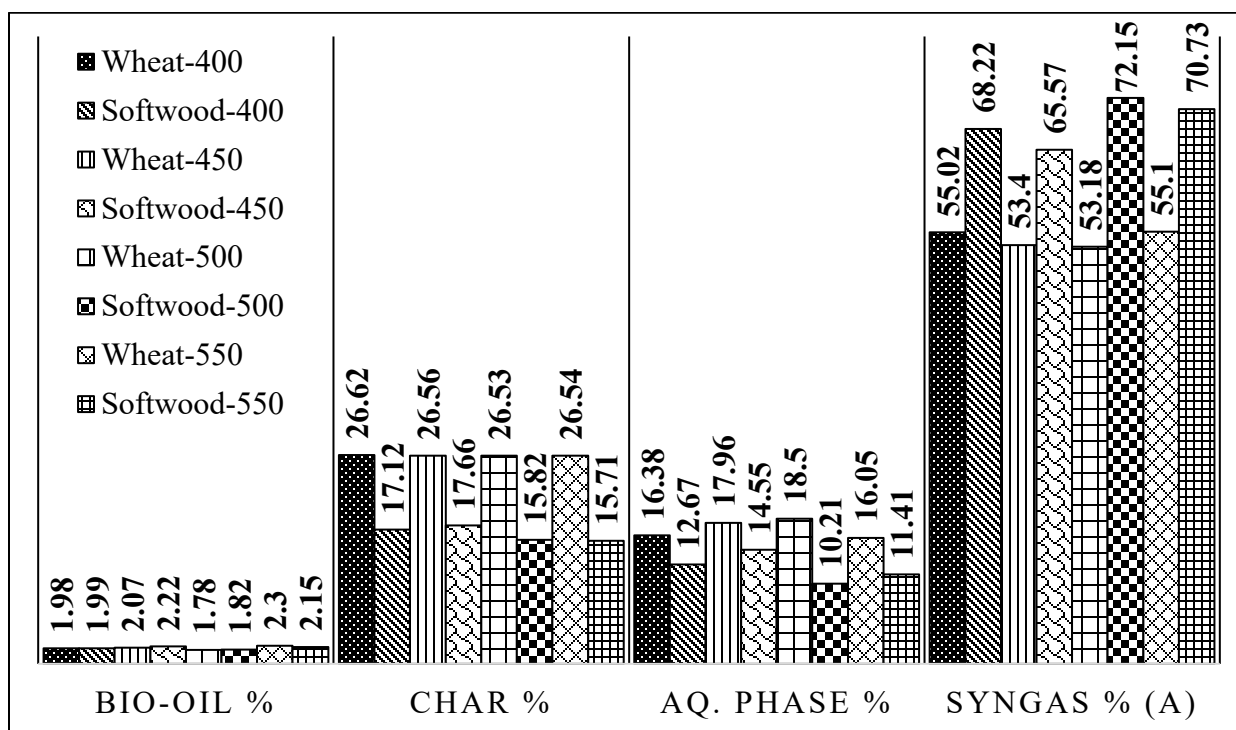


Figure 4.2 TCR product yields from softwood and wheat straw pellets at a fixed reformer temperature of 700 °C

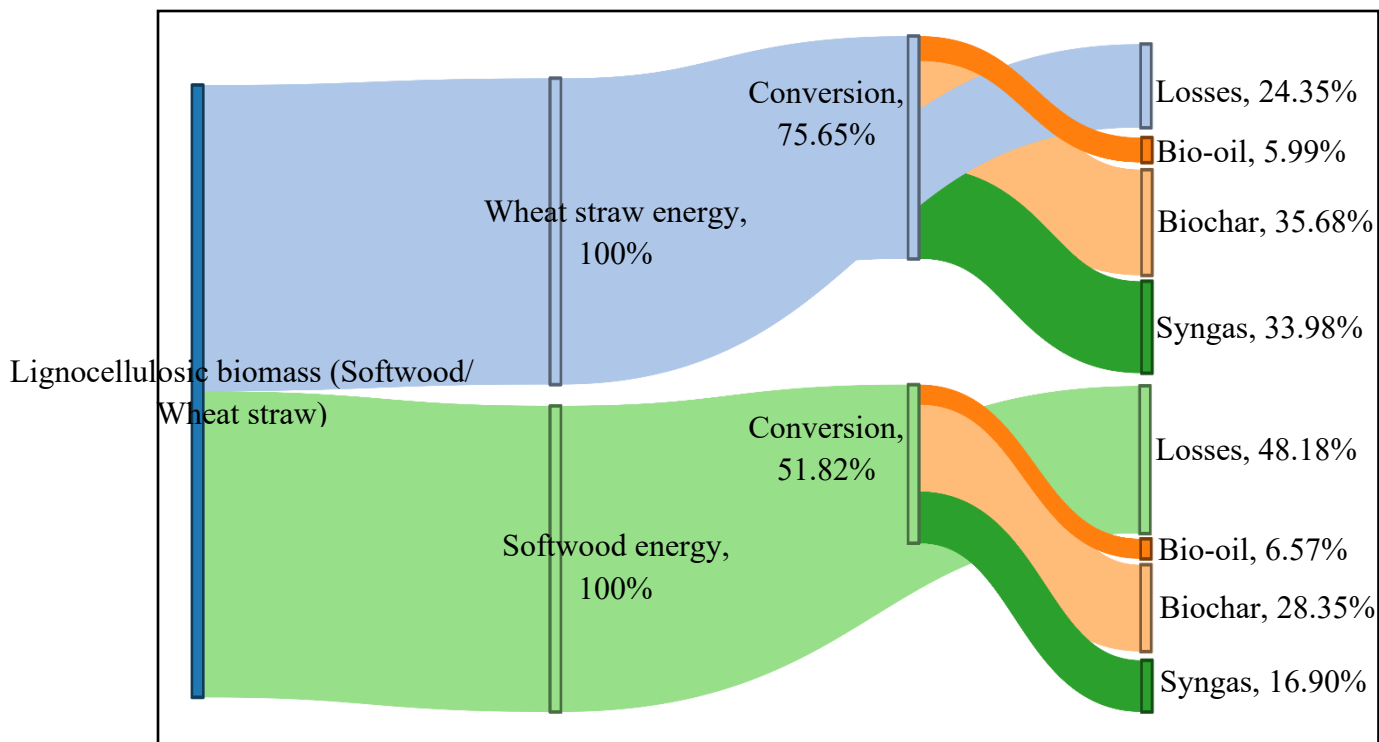


Figure 4.3 TCR energy conversion data for softwood and wheat straw pellets at 500 °C (reactor) and 600 °C (reformer)

TCR[®] energy conversion results for both wheat straw and softwood pellets at a reactor temperature of 500 °C and a reformer temperature of 600 °C are shown in the Sankey diagram in Figure 4.3. In total, 75.65% of the wheat straw pellet's energy is converted into a valorized form, and 24.35% of the feed energy was lost during the conversion in an aqueous phase and loss to the surroundings. In the case of softwood pellets, half of the available energy was lost during the conversion, and the rest of the energy was converted to bio-oil (6.57%), biochar (28.35%), and syngas (16.90%).

The viscosity, TAN, and HHV of bio-oil produced at a fixed reactor temperature of 400 °C and reformer temperatures of 500, 600, and 700 °C are shown in Figure 4.4. For all tested reformer temperatures, the TAN for the bio-oil from wheat straw pellet was more than five times that of oil produced from softwood pellets. The lowest TAN for each feedstock was obtained at a 700 °C reformer temperature. The lowest TAN obtained for wheat straw pellets was 56.7 mg KOH/g, whereas for softwood pellets, it was 8 mg KOH/g. Surprisingly, at 500 and 600 °C, the bio-oil

produced from softwood has a higher viscosity than that from wheat straw pellets; it is the opposite at a 700 °C reformer temperature. Irrespective of reformer temperature, the HHV of the bio-oil from softwood pellets was superior to that from wheat straw pellets. This mainly happening because of difference in carbon and hydrogen content in the bio-oil produced.

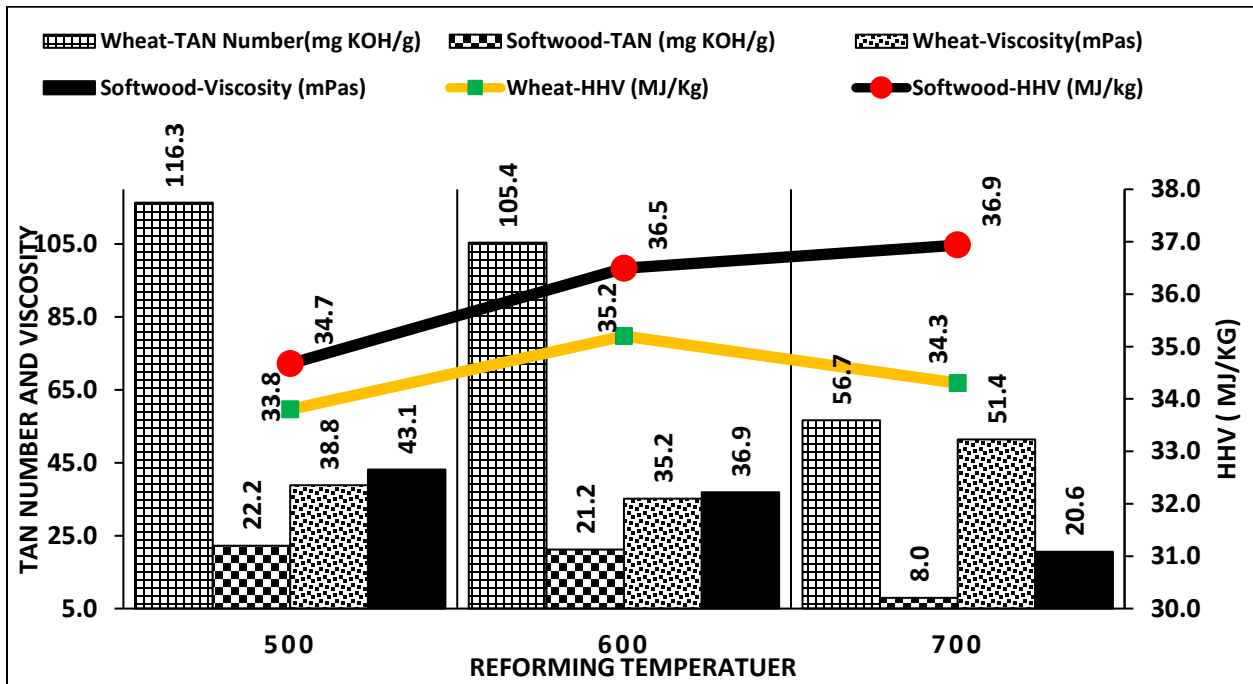


Figure 4.4 Viscosity, TAN, and HHV for wheat straw and softwood pellets at a fixed reactor temperature of 400 °C

The composition of syngas produced at reactor temperatures of 400 to 550 °C at a fixed reformer temperature of 700 °C for wheat straw pellets and softwood pellets is shown in Figure 4.5. Syngas produced from wheat straw pellets has a high concentration of hydrogen compared to that from softwood pellets at every reactor temperature. The highest value of hydrogen (36.29%) was obtained from wheat straw pellets at a 450 °C reactor temperature and the lowest (12.84%) was recorded for softwood pellets at a 550 °C reactor temperature. The HHV of syngas produced from softwood is significantly higher than the HHV obtained from wheat straw pellets because of the good proportions of CO, CH₄, and H₂ in the syngas.

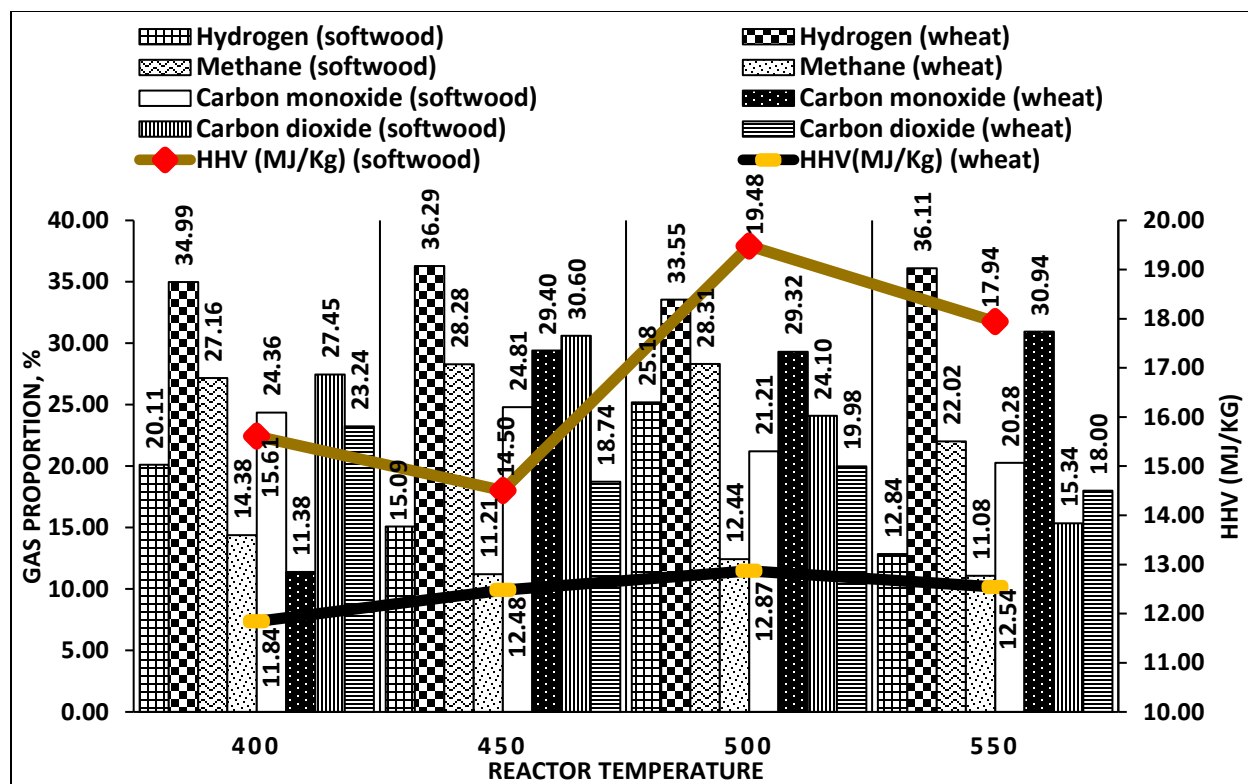


Figure 4.5 Syngas composition comparison for wheat straw and softwood pellets at a fixed reforming temperature of 700 °C.

4.2 Conclusions

The thermo-catalytic reforming of forest residue (softwood pellets) and agricultural residue (wheat straw pellets) produces combustible gases, high-quality bio-oil, and biochar. Syngas from softwood pellets contains hydrogen concentrations ranging from 10.46 to 25.18 vol.% and methane from 22.02 to 31.41 vol.%. Syngas from wheat straw pellets contains hydrogen from 21.01 to 36.29 vol.% and methane from 11.08 to 15.33 vol.%. The HHV of syngas produced from wheat straw pellets ranges from 8.16 to 12.87 MJ/Kg and, from softwood pellets, from 13.4 to 20.85 MJ/Kg. Bio-oil produced from softwood pellets has a very low TAN (22.2 to 3.14 mg KOH/g) and viscosity (50.9 to 11.9 mPas) and PAHs as high as 52.14%, O-compounds as low as 2.3%, and phenolic compounds as low as 16.40%. Bio-oil produced from wheat straw pellets has a TAN as low as 7.29 mg KOH/g, viscosity as low as 3.87 mPas, PAHs as high as 53.1%, O-compounds as

low as 2.7%, and phenolic compounds as low as 13.26%, which show the superior quality of bio-oil produced through TCR[®] compared to the traditional pyrolysis process. The biochar produced has very low O/C (0.054 for wheat and 0.477 for wheat straw) and H/C (0.0009 for softwood and 0.014 for wheat straw), indications of excellent stability.

The bio-oil yield was highest in both feedstocks studied at low reactor and reformer temperatures. Increasing either the reactor or the reformer temperature increases the total syngas yield and decreases the bio-oil and biochar yields. Thus, trade-offs need to be made between the quality and the quantity to determine optimal bio-oil conditions. Because of the significantly improved TAN, viscosity, and composition, it is concluded that at any operation condition studied, the bio-oil produced is significantly superior in quality to the bio-oil from other traditional pyrolysis processes regardless of the types of feedstocks used for this study.

The optimum temperatures recommended for bio-oil production from wheat straw pellets is 450 °C (reactor) and 600 °C (reformer). Though bio-oil yield at the 450-600 °C reactor-reformer temperature is moderate (3.83 wt.%), because of its significantly improved quality (a TAN of 33.98 mg KOH/g, viscosity of 41.97 mPas, HHV of 36 MJ/Kg, and less oxygen content (8.27%) than traditional oil), it is recommended over all other temperature sets tested. Similarly, for softwood pellets, 500 °C (reactor), 600 °C (reformer) temperatures are recommended. Total bio-oil yield at 500-600 °C, reactor-reformer temperature is 3.49 wt.%. Other properties like TAN (18.795 mg KOH/g), viscosity (43 mPas), HHV (36.40 MJ/Kg), and oxygen content (7.405%) are observed to be of good quality at the recommended temperature.

4.3 Recommendations for Future work

One forest residue feedstock (softwood pellets) and one agricultural residue feedstock (wheat straw pellets) were explored for the thermo-catalytic reforming experiments. Some of the future works on this TCR[®] unit would be to:

1. Test other feedstocks such as corn stover, canola straw, municipal solid waste, sewage sludge, etc., to produce biofuels using TCR[®] technology.
2. Investigate the effect of feedstock moisture content on the product yield and quality.
3. Study the influence of scale-up on TCR[®] technology and its products using a TCR-2 (2 kg/h unit) and a TCR-30 (30 kg/h unit).
4. Test the feeding of wood chips directly into the TCR[®] unit.
5. Testing of the biomass feedstocks should be carried out in a 30 kg/hr pilot scale TCR unit.
6. Techno-economic feasibility of using TCR[®] technology at municipal scale in a decentralized scale should be tested.

References

1. Environment and Climate Change Canada, Canadian Environmental Sustainability Indicators: Greenhouse gas emissions. Available from: www.canada.ca/en/environment-climate-change/services/environmental-indicators/greenhouse-gasemissions.html. [Accessed: 20 April 2021]
2. Natural Resource Canada, Energy Fact Book 2020-2021. Available from: https://www.nrcan.gc.ca/sites/nrcan/files/energy/energy_fact/energy_factbook-2020-2021-English.pdf. [Accessed: 20 April 2021]
3. U.S. Energy Information Administration, Biomass explained. Available from: <https://www.eia.gov/energyexplained/biomass/>. [Accessed: 21 April 2020]
4. Baruah, J., et al., Recent trends in the pretreatment of lignocellulosic biomass for value-added products. *Frontiers in Energy Research*, 2018. **6**: p. 141.
5. Acuna, M., et al., Methods to manage and optimize forest biomass supply chains: A review. *Current Forestry Reports*, 2019. **5**(3): p. 124-141.
6. Antar, M., et al., Biomass for a sustainable bioeconomy: An overview of world biomass production and utilization. *Renewable and Sustainable Energy Reviews*, 2021. **139**: p. 110691.
7. Natural Resources Canada, Forest Fact Book 2018-2019. Available from: <https://dl1ied5g1xfp8.cloudfront.net/pdfs/39505.pdf>. [Accessed: 2 March 2020]
8. Thakur, A., C.E. Canter, and A. Kumar, Life-cycle energy and emission analysis of power generation from forest biomass. *Applied energy*, 2014. **128**: p. 246-253.
9. Mupondwa, E., X. Li, and L. Tabil, Large-scale commercial production of cellulosic ethanol from agricultural residues: A case study of wheat straw in the Canadian Prairies. *Biofuels, Bioproducts and Biorefining*, 2017. **11**(6): p. 955-970.
10. Li, X., et al., A review of agricultural crop residue supply in Canada for cellulosic ethanol production. *Renewable and Sustainable Energy Reviews*, 2012. **16**(5): p. 2954-2965.
11. Anwar, Z., M. Gulfray, and M. Irshad, Agro-industrial lignocellulosic biomass a key to unlock the future bio-energy: a brief review. *Journal of radiation research and applied sciences*, 2014. **7**(2): p. 163-173.
12. Sawatdeenarunat, C., et al., Anaerobic digestion of lignocellulosic biomass: challenges and opportunities. *Bioresource Technology*, 2015. **178**: p. 178-186.
13. Limayem, A. and S.C. Ricke, Lignocellulosic biomass for bioethanol production: current perspectives, potential issues and future prospects. *Progress in energy and combustion science*, 2012. **38**(4): p. 449-467.
14. Kan, T., V. Strezov, and T.J. Evans, Lignocellulosic biomass pyrolysis: A review of product properties and effects of pyrolysis parameters. *Renewable and Sustainable Energy Reviews*, 2016. **57**: p. 1126-1140.
15. Chhiti, Y. and M. Kemiha, Thermal conversion of biomass, pyrolysis and gasification. *International Journal of Engineering and Science (IJES)*, 2013. **2**(3): p. 75-85.
16. Dhyani, V. and T. Bhaskar, A comprehensive review on the pyrolysis of lignocellulosic biomass. *Renewable energy*, 2018. **129**: p. 695-716.
17. Greenhalf, C., Thermochemical characterisation of various biomass feedstock and bio-oil generated by fast pyrolysis. 2014, Aston University.
18. Basu, P., Biomass gasification, pyrolysis and torrefaction: practical design and theory. 2018: Academic press.

19. Panwar, N., R. Kothari, and V. Tyagi, Thermo chemical conversion of biomass–Eco friendly energy routes. *Renewable and Sustainable Energy Reviews*, 2012. **16**(4): p. 1801-1816.
20. Hornung, A., *Biomass combustion science, technology and engineering: 8. Intermediate pyrolysis of biomass*. 2013: Elsevier Science.
21. Mahmood, A.S., et al., The intermediate pyrolysis and catalytic steam reforming of Brewers spent grain. *Journal of Analytical and Applied Pyrolysis*, 2013. **103**: p. 328-342.
22. Sharifzadeh, M., et al., The multi-scale challenges of biomass fast pyrolysis and bio-oil upgrading: Review of the state of art and future research directions. *Progress in Energy and Combustion Science*, 2019. **71**: p. 1-80.
23. Achinas, S., An Overview of the Technological Applicability of Plasma Gasification Process, in *Contemporary Environmental Issues and Challenges in Era of Climate Change*. 2020, Springer. p. 261-275.
24. Andreas, A., et al., Thermo-Catalytic Reforming of Woody Biomass. *Energy & Fuels*, 2016.
25. Ahmad, E., et al., Integrated thermo-catalytic reforming of residual sugarcane bagasse in a laboratory scale reactor. *Fuel Processing Technology*, 2018. **171**: p. 277-286.
26. Korres, N.E., et al., Bioenergy production by anaerobic digestion : using agricultural biomass and organic wastes. xxx, 442 pages.
27. Brandt, A., et al., Deconstruction of lignocellulosic biomass with ionic liquids. *Green chemistry*, 2013. **15**(3): p. 550-583.
28. Hassan, S.S., G.A. Williams, and A.K. Jaiswal, Emerging technologies for the pretreatment of lignocellulosic biomass. *Bioresource Technology*, 2018. **262**: p. 310-318.
29. The Paris agreement on climate change. 11-2019 7/16/2019]; Available from: <https://www.nrdc.org/sites/default/files/paris-agreement-climate-change-2017-ib.pdf>.
30. Progress towards Canada’s greenhouse gas emissions reduction target Canadian environmental sustainability indicators. Available from: <https://www.canada.ca/content/dam/eccc/documents/pdf/cesindicators/progress-towards-canada-greenhouse-gas-reduction-target/2021/progress-ghg-emissions-reduction-target.pdf>. [Accessed: 7 May 2021]
31. Energy Fact Book 2020-2021. Available from: https://www.nrcan.gc.ca/sites/nrcan/files/energy/energy_fact/energy-factbook-2020-2021-English.pdf. [Accessed: 11 May 2021]
32. Zheng, Y. and F. Qiu, Bioenergy in the Canadian Prairies: Assessment of accessible biomass from agricultural crop residues and identification of potential biorefinery sites. *Biomass and Bioenergy*, 2020. **140**: p. 105669.
33. Zhao, S. and Y. Luo, Multiscale Modeling of Lignocellulosic Biomass Thermochemical Conversion Technology: An Overview on the State-of-the-Art. *Energy & Fuels*, 2020. **34**(10): p. 11867-11886.
34. Schmitt, N., et al., Thermo-chemical conversion of biomass and upgrading to biofuel: The Thermo-Catalytic Reforming process–A review. *Biofuels, Bioproducts and Biorefining*, 2019. **13**(3): p. 822-837.
35. Government of Canada, Gratification. Available from: <https://www.nrcan.gc.ca/energy/energy-sources-distribution/coal-and-co2-capture-storage/gasification/4355>. [Accessed: 11 May 2021]

36. Ibarra-Gonzalez, P. and B.-G. Rong, A review of the current state of biofuels production from lignocellulosic biomass using thermochemical conversion routes. *Chinese Journal of Chemical Engineering*, 2019. **27**(7): p. 1523-1535.
37. Conti, R., et al., Thermocatalytic reforming of biomass waste streams. *Energy Technology*, 2017. **5**(1): p. 104-110.
38. Marazza, D., et al., Greenhouse gas savings and energy balance of sewage sludge treated through an enhanced intermediate pyrolysis screw reactor combined with a reforming process. *Waste Management*, 2019. **91**: p. 42-53.
39. Santos, J., et al., Integrated intermediate catalytic pyrolysis of wheat husk. *Food and Bioproducts Processing*, 2019. **114**: p. 23-30.
40. Neumann, J., et al. Hydrodeoxygenation of Bio-oils from Thermo-Catalytic Reforming–High Energy Efficient Route to Renewable Gasoline and Diesel. in 24th European Biomass Conference: Setting the course for a biobased economy. Extracted from the Proceedings of the International Conference held in Amsterdam, The Netherlands, Amsterdam, Florence, Italy. 2016.
41. Yang, Y., et al., Intermediate pyrolysis of biomass energy pellets for producing sustainable liquid, gaseous and solid fuels. *Bioresource technology*, 2014. **169**: p. 794-799.
42. Ahmad, E., et al., Integrated thermo-catalytic reforming of residual sugarcane bagasse in a laboratory scale reactor. *Fuel Processing Technology*, 2018. **171**: p. 277-286.
43. Neumann, J., et al., The conversion of anaerobic digestion waste into biofuels via a novel thermo-catalytic reforming process. *Waste Management*, 2016. **47**: p. 141-148.
44. Neumann, J., et al., Production and characterization of a new quality pyrolysis oil, char and syngas from digestate–Introducing the thermo-catalytic reforming process. *Journal of Analytical and Applied Pyrolysis*, 2015. **113**: p. 137-142.
45. Jäger, N., et al., Thermo-catalytic reforming of woody biomass. *Energy & Fuels*, 2016. **30**(10): p. 7923-7929.
46. Ouadi, M., et al., Thermo-catalytic reforming of co-form® rejects (waste cleansing wipes). *Journal of Analytical and Applied Pyrolysis*, 2018. **132**: p. 33-39.
47. Ouadi, M., et al., Thermo-catalytic reforming of pulper rejects from a secondary fibre mill. *Renewable Energy Focus*, 2018. **26**: p. 39-45.
48. Ouadi, M., et al., Thermo-Catalytic Reforming of municipal solid waste. *Waste Management*, 2017. **68**: p. 198-206.
49. ASAE Standards for Moisture Determination. Available from: <https://engineering.purdue.edu/~abe305/moisture/html/page13.htm>. [Accessed: 30 August 2021]
50. Standard Test Methods for Proximate Analysis of Coal and Coke by Macro Thermogravimetric Analysis. Available from: <https://www.astm.org/Standards/D7582.htm>. [Accessed: 30 August 2021]
51. Standard Test Method for Carbon and Hydrogen in the Analysis Sample of Refuse-Derived Fuel. Available from: <https://www.astm.org/Standards/E777.htm>. [Accessed: 30 August 2021]
52. Standard Test Methods for Nitrogen in Refuse-Derived Fuel Analysis Samples. Available from: <https://standards.globalspec.com/std/9956413/ASTM%20E778>. [Accessed: 30 August 2021]

53. Standard Test Methods for Total Sulfur in the Analysis Sample of Refuse-Derived Fuel. Available from: <https://standards.globalspec.com/std/9956433/ASTM%20E775>. [Accessed: 30 August 2021]
54. Gill, M., et al., Thermo-catalytic reforming of alberta-based biomass feedstock to produce biofuels. *Biomass and Bioenergy*, 2021. **152**: p. 106203.
55. Standard Test Method for Shear Viscosity of Coal-Tar and Petroleum Pitches. Available from: [document-center.com/standards/show/ASTM-D5018](https://www.astm.org/standards/show/ASTM-D5018). [Accessed: 30 August 2021]
56. Standard Test Method for Acid Number of Petroleum Products by Potentiometric Titration. Available from: <https://www.astm.org/DATABASE.CART/HISTORICAL/D664-04.htm>. [Accessed: 30 August 2021]
57. Elmously, M., et al., Thermo-Catalytic Reforming of spent coffee grounds. *Bioresources and Bioprocessing*, 2019. **6**(1): p. 1-12.
58. Gill, M.K., Thermo-catalytic reforming of woody biomass, Master of science in Chemical Engineering. 2020, University of Alberta: Edmonton.
59. Environment and Climate Change Canada, Greenhouse Gas Emissions Environmental Sustainability Indicators. Available from: <https://www.canada.ca/content/dam/eccc/documents/pdf/cesindicators/ghg-emissions/2020/greenhouse-gas-emissions-en.pdf>. [Accessed: 14 July 2021]
60. Natural Resource Canada, Energy Fact Book 2019-2020. Available from: https://www.nrcan.gc.ca/sites/www.nrcan.gc.ca/files/energy/pdf/Energy%20Fact%20Book%202019%202020_web-resolution.pdf. [Accessed: 14 July 2021]
61. Wu, Z., et al., Co-pyrolysis of lignocellulosic biomass with low-quality coal: optimal design and synergistic effect from gaseous products distribution. *Fuel*, 2019. **236**: p. 43-54.
62. Goyal, H., D. Seal, and R. Saxena, Bio-fuels from thermochemical conversion of renewable resources: a review. *Renewable and sustainable energy reviews*, 2008. **12**(2): p. 504-517.
63. Wang, S., et al., Lignocellulosic biomass pyrolysis mechanism: a state-of-the-art review. *Progress in Energy and Combustion Science*, 2017. **62**: p. 33-86.
64. Funke, A., et al., Experimental comparison of two bench scale units for fast and intermediate pyrolysis. *Journal of Analytical and Applied Pyrolysis*, 2017. **124**: p. 504-514.
65. Huber, G.W., S. Iborra, and A. Corma, Synthesis of transportation fuels from biomass: chemistry, catalysts, and engineering. *Chemical reviews*, 2006. **106**(9): p. 4044-4098.
66. Kirby, M.E., et al., The role of thermo-catalytic reforming for energy recovery from food and drink supply chain wastes. *Energy Procedia*, 2017. **123**: p. 15-21.
67. Elmously, M., et al., Upscaling of thermo-catalytic reforming process from lab to pilot scale. *Industrial & Engineering Chemistry Research*, 2019. **58**(35): p. 15853-15862.
68. Elmously, M., et al., Thermo-Catalytic Reforming of spent coffee grounds. *Bioresources and Bioprocessing*, 2019. **6**(1): p. 44.
69. Ouadi, M., et al., Food and market waste—A pathway to sustainable fuels and waste valorization. *Energy & Fuels*, 2019. **33**(10): p. 9843-9850.
70. Channiwala, S. and P. Parikh, A unified correlation for estimating HHV of solid, liquid and gaseous fuels. *Fuel*, 2002. **81**(8): p. 1051-1063..

71. Neumann, J., et al., Production and characterization of a new quality pyrolysis oil, char and syngas from digestate – Introducing the thermo-catalytic reforming process. *Journal of Analytical and Applied Pyrolysis*, 2015. **113**: p. 137-142.

Appendix A

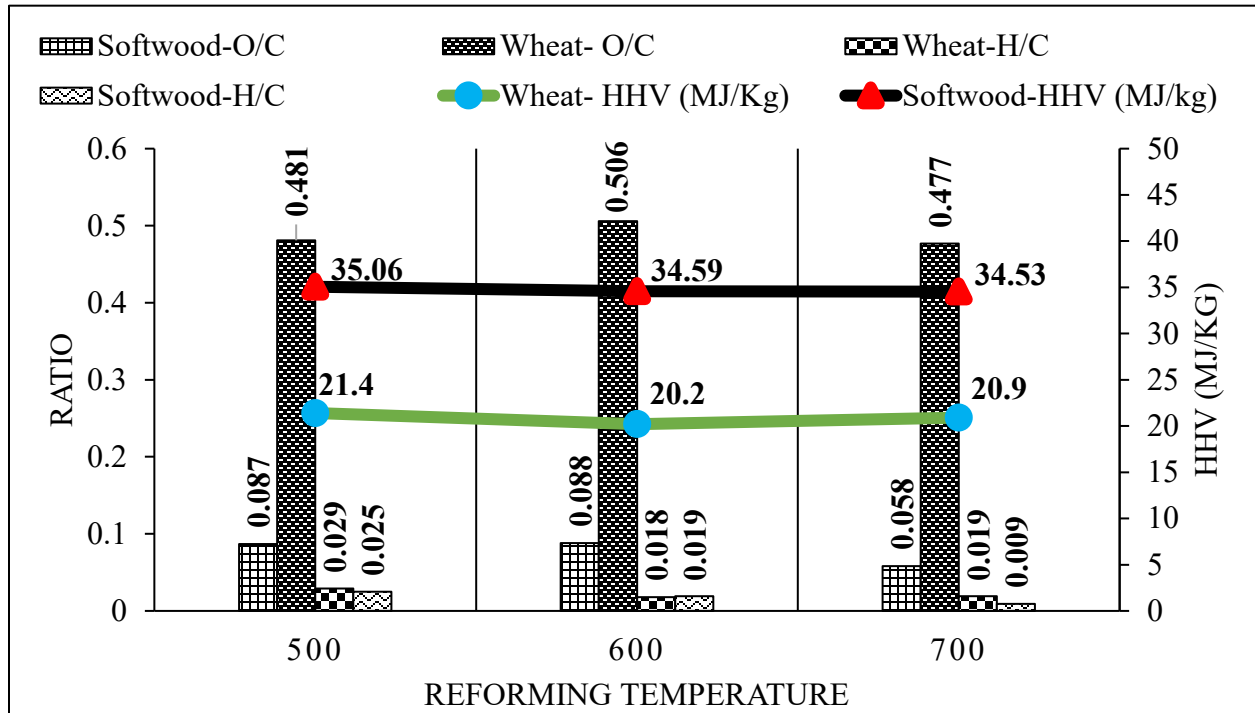


Figure A- 2 Softwood and Wheat residue pellets biochar comparison at a fixed reactor temperature of 400°C

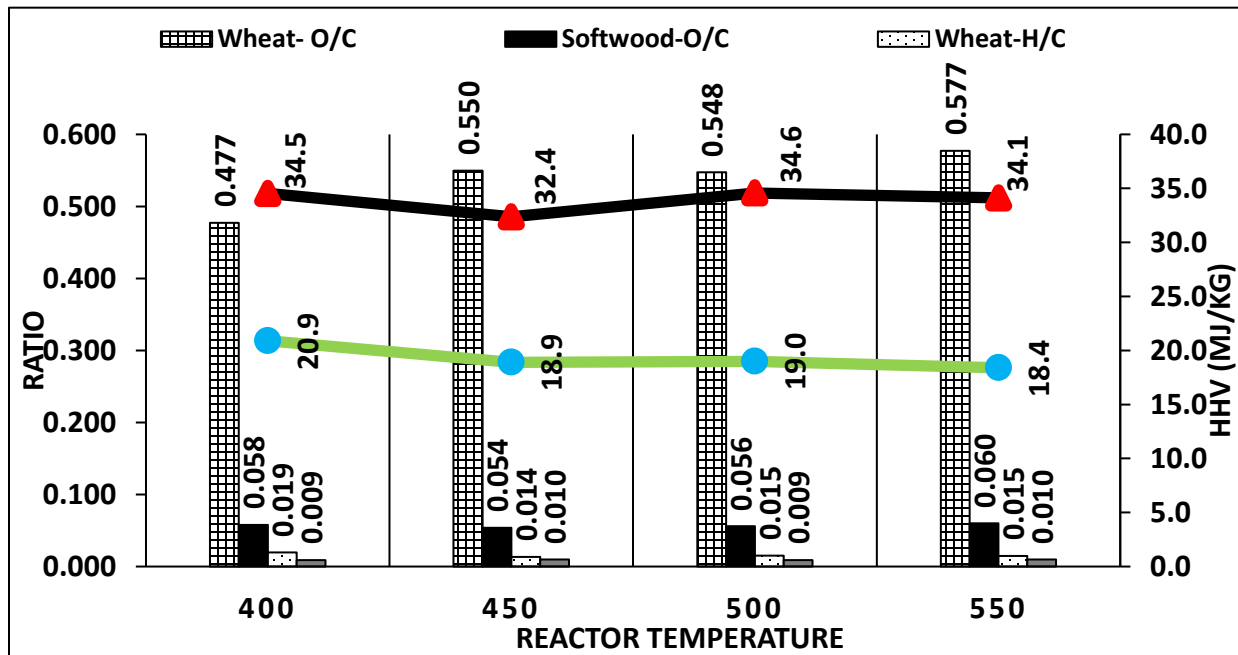


Figure A- 3 Softwood and Wheat residue pellets biochar comparison at fixed reformer temperature of 700°C

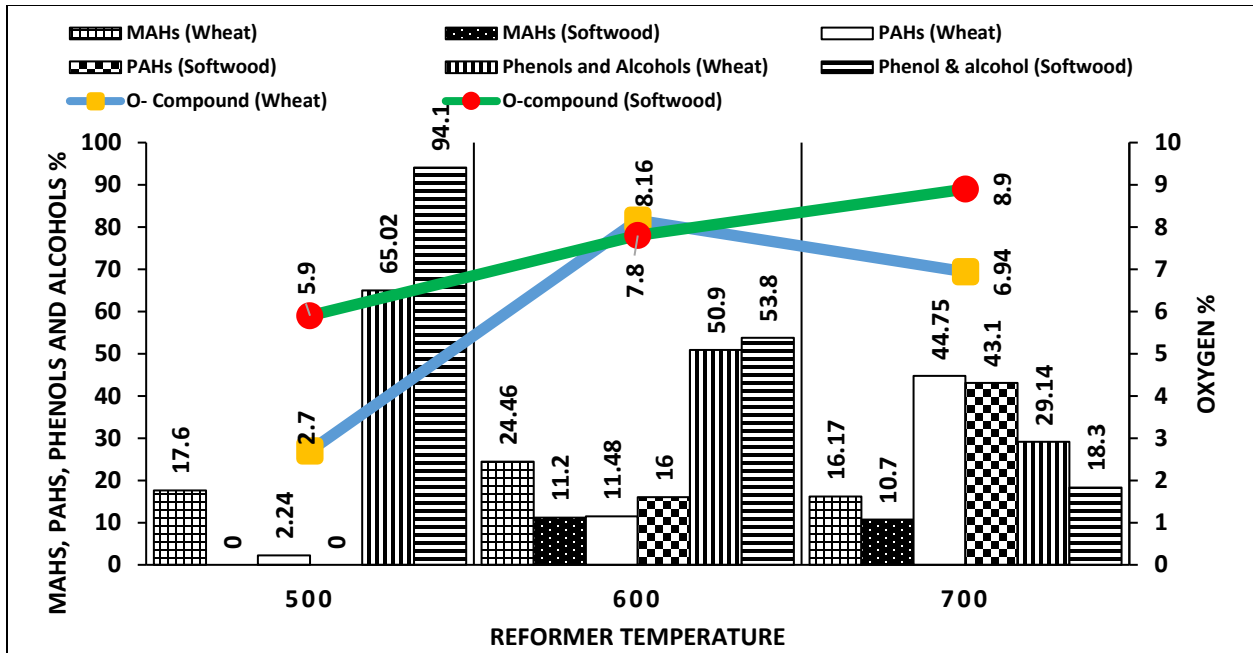


Figure A- 4 Comparison of GCMS analysis of wheat residue and softwood pellets at a fixed reactor temperature of 400 °C.

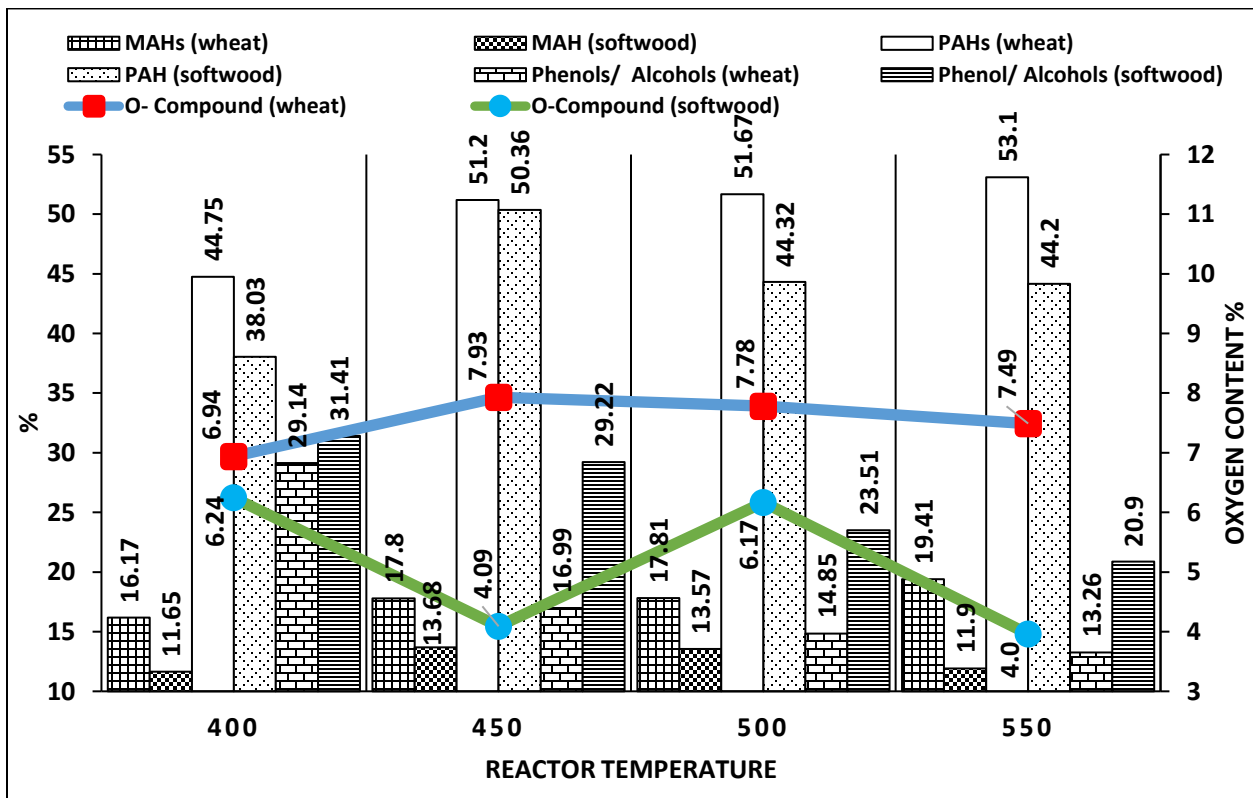


Figure A- 5 Comparison of GCMS analysis of wheat residue and softwood pellets at a fixed reformer temperature of 700 °C.

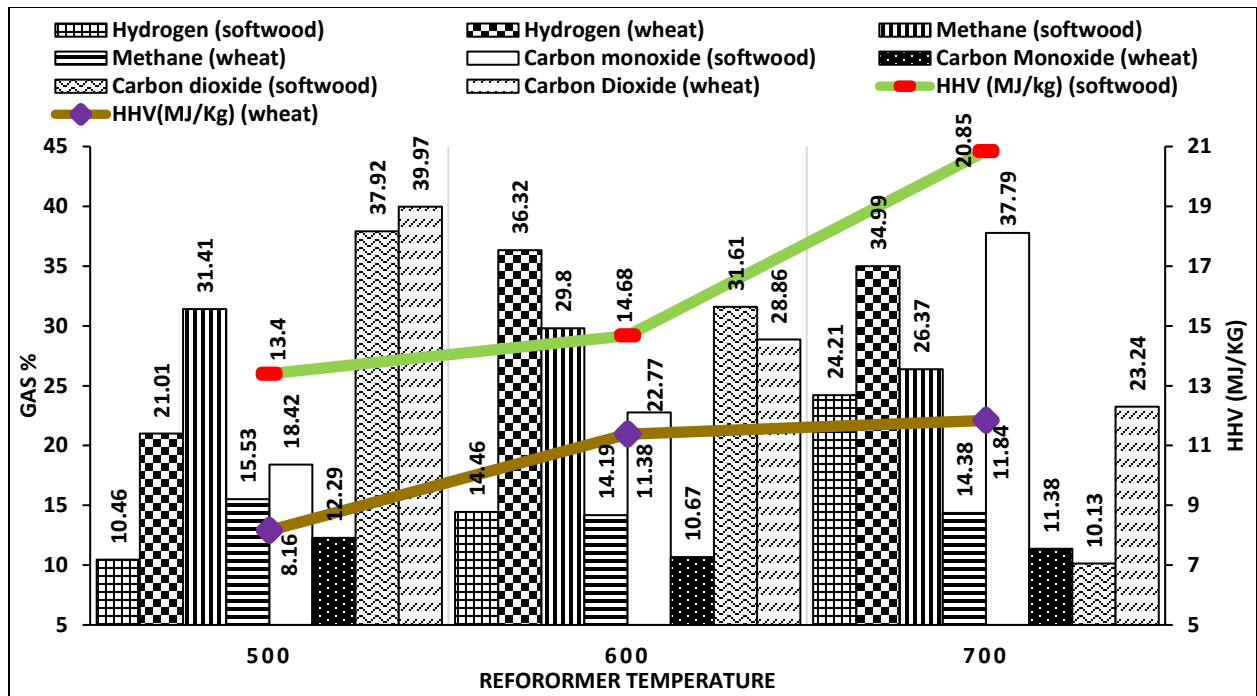


Figure A- 6 Syngas proportion comparison softwood and wheat residue pellets